
SIZE-INVARIANT GRAPH REPRESENTATIONS FOR GRAPH CLASSIFICATION EXTRAPOLATIONS

A PREPRINT

Beatrice Bevilacqua

Department of Computer Science
Purdue University
bbevilac@purdue.edu

Yangze Zhou

Department of Statistics
Purdue University
zhou950@purdue.edu

Bruno Ribeiro

Department of Computer Science
Purdue University
ribeiro@cs.purdue.edu

June 14, 2022

ABSTRACT

In general, graph representation learning methods assume that the test and train data come from the same distribution. In this work we consider an underexplored area of an otherwise rapidly developing field of graph representation learning: The task of out-of-distribution (OOD) graph classification, where train and test data have different distributions, with test data unavailable during training. Our work shows it is possible to use a causal model to learn approximately invariant representations that better extrapolate between train and test data. Finally, we conclude with synthetic and real-world dataset experiments showcasing the benefits of representations that are invariant to train/test distribution shifts.

Keywords Graph Representation Learning · Graph Neural Networks · Graph Classification · Causal Extrapolation

1 Introduction

In general, graph representation learning methods assume that the test and train data come from the same distribution. Unfortunately, this assumption is not always valid in real-world deployments [57, 68, 31]. When the test distribution is different from training, the test data is described as *out of distribution (OOD)*. Differences in train/test distribution may be due to environmental factors such as those related to the way the data is collected or processed.

Particularly, in graph classification tasks, where \mathcal{G} is the graph and Y its label, we often see different graph sizes and/or distinct arrangements of vertex attributes associated with the same target label. *How should we learn a graph representation for out-of-distribution inductive tasks (extrapolations), where the graphs in training and test (deployment) have distinct characteristics (i.e., $P^{tr}(\mathcal{G}) \neq P^{te}(\mathcal{G})$)?* Are inductive graph neural networks (GNNs) robust to distribution shifts between $P^{tr}(\mathcal{G})$ and $P^{te}(\mathcal{G})$? If not, is it possible to design a graph classifier that is robust to such OOD shifts without access to samples from $P^{te}(\mathcal{G})$?

In this work we consider an OOD graph classification task with different train and test distributions based on graph sizes and vertex attributes. Our work focuses on simple (no self-loops) undirected graphs with discrete vertex attributes. We make the common assumption of independence between cause and mechanisms [17, 19, 58, 77, 103, 112, 7], which states that $P(Y|\mathcal{G})$ remains the same between train and test. We also assume we do not have access to samples from $P^{te}(\mathcal{G})$, hence covariate shift adaptation methods (such as Yehudai et al. [146]) are unfit for our scenario. In our setting we need to learn to extrapolate from a causal model.

Contributions. Our contributions are as follows:

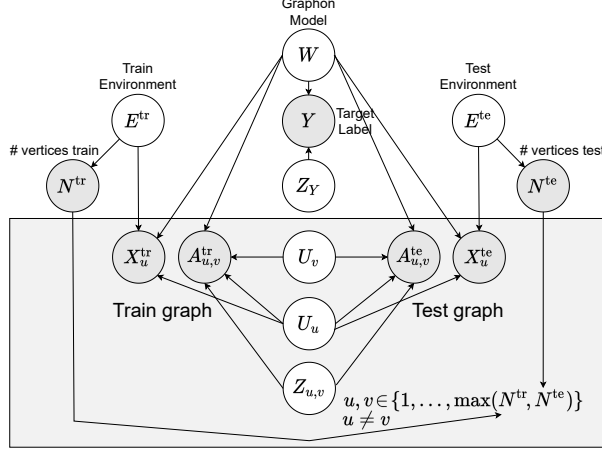


Figure 1: The twin network DAG [11] of our structural causal model (SCM). Gray (resp. white) vertices represent observed (resp. hidden) random variables.

1. We provide a causal model that formally describes a class of graph classification tasks where the training ($P^{tr}(\mathcal{G})$) and test ($P^{te}(\mathcal{G})$) graphs have different size and vertex attribute distributions.
2. Assuming independence between cause and mechanism (ICM) [77, 114], we introduce a graph representation method based on the work of Lovász and Szegedy [79] and Graph Neural Networks (GNNs) [65, 50, 147] that is invariant to the train/test distribution shifts of our causal model. Unlike existing invariant representations, this representation can perform extrapolations from single training environment (e.g., all training graphs have the same size).
3. Our empirical results show that, in most experiments, neither Invariant Risk Minimization (IRM) [7] nor the GNN extrapolation modifications proposed by Xu et al. [143] are able to perform well in graph classification tasks over the OOD test data.

2 Graph Classification: A Causal Model Based on Random Graphs

Out-of-distribution (OOD) shift. For any joint distribution $P(Y, \mathcal{G})$ of graphs \mathcal{G} and labels Y , there are infinitely many causal models that give the same joint distribution [97]. This phenomenon is known as model underspecification. Hence, if the training data distribution $P^{tr}(Y, \mathcal{G})$ does not have the same support as the test distribution $P^{te}(Y, \mathcal{G})$, a model trained with samples drawn from $P^{tr}(Y, \mathcal{G})$ needs to be able to extrapolate in order to correctly predict $P^{te}(Y|\mathcal{G})$. In this work, we assume Independence between Cause and Mechanism (ICM): $P^{tr}(Y|\mathcal{G}) = P^{te}(Y|\mathcal{G})$, which is a common assumption in the causal deep learning literature [17, 19, 58, 77, 103, 112, 7].

In inductive graph classification tasks, ICM implies that the shift between train and test distributions $P^{tr}(Y, \mathcal{G}) \neq P^{te}(Y, \mathcal{G})$ comes from $P^{tr}(\mathcal{G}) \neq P^{te}(\mathcal{G})$, since $P^{tr}(Y|\mathcal{G}) = P^{te}(Y|\mathcal{G})$. And because our task is inductive, i.e., no data from $P^{te}(\mathcal{G})$ or a proxy variable, we must make assumptions about the causal mechanisms in order to extrapolate.

Causal model. A graph representation that is robust (invariant) to shifts in $P^{te}(\mathcal{G})$ must know how the distribution shifts. Either it is given some examples from $P^{te}(\mathcal{G})$ (a.k.a. covariate shift adaptation [124], which is not out scenario) or be given a causal structure that describes how the test distribution can shift. Our paper focuses on the latter by giving a Structural Causal Model (SCM) for the data generation process. Figure 1 depicts the Directed Acyclic Graph (DAG) of our causal model. It uses the twin network DAGs structure first proposed by Balke and Pearl [11] (see Pearl [97, Chapter 7.1.4]) in order to define counterfactual queries.

In what follows we detail the SCM in Definitions 1 and 2. Our causal model is inspired by Stochastic Block Models (SBMs) [35, 119] and their connection to graphon random graph models [3, 79]:

Definition 1 (Training Graph $\mathcal{G}_{N^{tr}}^{tr}$). *The training graph SCM is depicted at the left side of the twin network DAG in Figure 1.*

- *The training graph is characterized by a sampled graphon $W \sim P(W)$, where $W : [0, 1]^2 \rightarrow [0, 1]$ is a random symmetric measurable function [79] sampled (according to some distribution) from \mathbb{D}_W , the set of all symmetric*

measurable functions on $[0, 1]^2 \rightarrow [0, 1]$. W defines both the graph's target label and some of its structural and attribute characteristics.

- The **training environment** $E^{tr} \sim P^{tr}(E)$ is a hidden environment variable that represents specific graph properties that change between the training and test. $E^{tr} \in \mathbb{E}$ for some properly defined environment space \mathbb{E} .
- The graph's size is determined by its environment $N^{tr} := \eta(E^{tr})$, where η is an unknown deterministic function.
- The graph's target label is given by $Y := h(W, Z_Y)$, $Y \in \mathbb{Y}$, with \mathbb{Y} some properly defined discrete target space. Z_Y is an independent random noise variable and h is a deterministic function on the input space $\mathbb{D}_W \times \mathbb{R}$.
- The vertices are numbered $V^{tr} = \{1, \dots, N^{tr}\}$. Each vertex $v \in V^{tr}$ has an associated hidden variable $U_v \sim \text{Uniform}(0, 1)$ sampled i.i.d.. The graph is undirected and its adjacency matrix $A^{tr} \in \{0, 1\}^{N^{tr} \times N^{tr}}$ is defined by

$$A_{u,v}^{tr} := \mathbb{1}(Z_{u,v} > W(U_u, U_v)), \forall u, v \in V^{tr}, u \neq v. \quad (1)$$

The diagonals are set to 0 because there is no self-loop. Here $\mathbb{1}$ is an indicator function, and $\{Z_{u,v} = Z_{v,u}\}_{u,v \in V^{tr}}$ are independent uniform noises on $[0, 1]$.

- The graph may contain discrete vertex attributes $X^{tr} \in \mathbb{X}^{N^{tr}}$ defined as

$$X_v^{tr} := g_X(E^{tr}, W(U_v, U_v)), \forall v \in V^{tr},$$

where $X_v^{tr} \in \mathbb{X}$, and \mathbb{X} is some properly defined attribute space. g_X is a deterministic function that determines a vertex attribute using $W(U_v, U_v) \in [0, 1]$ via, say, inverse sampling [130] the vertex attribute distribution.

- Then the training graph is described as

$$\mathcal{G}_{N^{tr}}^{tr} := (A^{tr}, X^{tr}).$$

The test data comes from the following (coupled) distribution, that is, the model uses some of the same random variables of the training graph model, effectively only replacing E^{tr} by E^{te} , as shown in the DAG of Figure 1.

Definition 2 (Test Graph $\mathcal{G}_{N^{te}}^{te}$). *The SCM of the test graph is given by the right side of the twin network DAG in Figure 1, changing the following variables from Definition 1:*

- The **test environment** $E^{te} \sim P^{te}(E)$, and $E^{te} \in \mathbb{E}$ belongs to the same space as E^{tr} . It represents specific properties of the graphs that change between the test and training data. Denote $\text{supp}(\cdot) := \{x | P(x) > 0\}$ as the support of a random variable. The supports of E^{te} and E^{tr} may not overlap (i.e., $\text{supp}(E^{te}) \cap \text{supp}(E^{tr}) = \emptyset$).
- The change in environment from E^{tr} to E^{te} may change the graph's size as $N^{te} := \eta(E^{te})$, where η is the same unknown deterministic function as in Definition 1.
- The vertices are numbered $V^{te} = \{1, \dots, N^{te}\}$. The adjacency matrix $A^{te} \in \{0, 1\}^{N^{te} \times N^{te}}$ is defined as in Equation (1).
- The graph may contain discrete vertex attributes $X^{te} \in \mathbb{X}^{N^{te}}$ defined as

$$X_v^{te} := g_X(E^{te}, W(U_v, U_v)), \forall v \in V^{te},$$

with g_X as given in Definition 1.

- Then the test graph is described as

$$\mathcal{G}_{N^{te}}^{te} := (A^{te}, X^{te}).$$

Our SCM has a direct connection with graphon random graph model [79], and extend it by considering vertex attributes. Now we introduce examples of our graph classification tasks based on Definitions 1 and 2 using two classic random graph models.

Notation: $(\mathcal{G}_{N^*}^*, E^*, A^*, V^*, X^*)$ In what follows we use the superscript $*$ as a wildcard to describe both train and test random variables. For instance, $\mathcal{G}_{N^*}^*$ is a variable that is a wildcard for referring to either $\mathcal{G}_{N^{tr}}^{tr}$ or $\mathcal{G}_{N^{te}}^{te}$. Also, from now on we define $P^{te}(\mathcal{G}) = P(\mathcal{G}_{N^{te}}^{te})$ and $P^{tr}(\mathcal{G}) = P(\mathcal{G}_{N^{tr}}^{tr})$.

Erdős-Rényi example. Consider a random training environment E^{tr} such that $N^{\text{tr}} = \eta(E^{\text{tr}})$ is the number of vertices for graphs in our training data. Let p be the probability that any two distinct vertices of the graph have an edge. Define W as a constant function that always outputs p . Sample independent uniform noises $Z_{u,v} \sim \text{Uniform}(0, 1)$ (for each possible edges, $Z_{u,v} = Z_{v,u}$). An Erdős-Rényi graph can be defined as a graph whose adjacency matrix A^{tr} is $A_{u,v}^{\text{tr}} = \mathbb{1}(Z_{u,v} > W(U_u, U_v)) = \mathbb{1}(Z_{u,v} > p)$, $\forall u, v \in V^{\text{tr}}, u \neq v$. Here vertex attributes are not considered and can define $X_v^{\text{tr}} = , \forall v \in V^{\text{tr}}$ as the null attribute.

In the test data, we have a different environment E^{te} and graph sizes $N^{\text{te}} = \eta(E^{\text{te}})$, with $\text{supp}(N^{\text{te}}) \cap \text{supp}(N^{\text{tr}}) = \emptyset$. The variable $\{Z_{u,v}\}_{u,v \in \{1, \dots, \max(\text{supp}(N^{\text{tr}}) \cup \text{supp}(N^{\text{te}}))\}}$ can be thought as the seed of a random number generator to determine if two distinct vertices u and v are connected by an edge. The above defines our training and test data as a set of Erdős-Rényi random graphs of sizes N^{tr} and N^{te} with probability p . The targets of the Erdős-Rényi graphs can be, for instance, the value $Y = p$ in Definition 1, which is determined by W and invariant of graph sizes.

Stochastic Block Model (SBM) [119]. A SBM can be seen as a generalization of Erdos-Renyi graphs. SBMs partition the vertex set into disjoint subsets S_1, S_2, \dots, S_r (known as blocks or communities) with an associated $r \times r$ symmetric matrix \mathbf{P} , where the probability of an edge (u, v) , $u \in S_i$ and $v \in S_j$ is P_{ij} , for $i, j \in \{1, \dots, r\}$. In the training and test data, we still have i.i.d sampled $Z_{u,v} = Z_{v,u}$ and different environments $E^{\text{tr}}, E^{\text{te}}$. Divide the interval $[0, 1]$ into disjoint convex sets $[t_0, t_1), [t_1, t_2), \dots, [t_{r-1}, t_r]$, where $t_0 = 0$ and $t_r = 1$, such that if $U_v \sim \text{Uniform}(0, 1)$ satisfies $U_v \in [t_{i-1}, t_i)$, then vertex v belongs to block S_i . Thus $W(U_u, U_v) = \sum_{i,j \in \{1, \dots, r\}} P_{ij} \mathbb{1}(U_u \in [t_{i-1}, t_i)) \mathbb{1}(U_v \in [t_{j-1}, t_j))$. A SBM graph in train or test can be defined as a graph whose adjacency matrix A^* is $A_{u,v}^* = \mathbb{1}(Z_{u,v} > W(U_u, U_v))$, $\forall u, v \in V^*$, $u \neq v$. Now we have a set of SBM random graphs of sizes N^{tr} and N^{te} with \mathbf{P} . Consider if there are only two blocks, the target Y can be $P_{1,2}$ which is the probability of an edge connecting between blocks. It is determined by W and invariant of graph sizes.

SBM with vertex attributes. For the SBM, assume the vertex attributes are tied to blocks, and are distinct for each block. The environment variable operates on changing the distributions of attributes assigned in each block. Consider the following SBM example with two blocks: Define $W(U_v, U_v) = \frac{U_v}{2t_1} \mathbb{1}(U_v \in [0, t_1)) + (\frac{1}{2} + \frac{U_v - t_1}{2(1-t_1)}) \mathbb{1}(U_v \in [t_1, 1])$. So $W(U_v, U_v) < \frac{1}{2}$ if and only if v belongs to the first block. We only change the values of W for points on a zero-measure space. Let g_X be such that it defines constants $0 < \alpha_{E^*,1} < \frac{1}{2} < \alpha_{E^*,2} < 1$, and vertex attributes as

$$X_v^* = g_X(E^*, W(U_v, U_v)) = \begin{bmatrix} \mathbb{1}(W(U_v, U_v) \in [0, \alpha_{E^*,1})) \\ \mathbb{1}(W(U_v, U_v) \in [\alpha_{E^*,1}, .5)) \\ \mathbb{1}(W(U_v, U_v) \in [.5, \alpha_{E^*,2})) \\ \mathbb{1}(W(U_v, U_v) \in [\alpha_{E^*,2}, 1]) \end{bmatrix},$$

where the attribute of vertex v , X_v^* , is one-hot encoded to represent 4 colors: red and blue (if v is in block 1) and green and yellow (if v is in block 2).

3 E-Invariant Graph Representations

In this section we discuss shortcomings of traditional graph representation methods on out-of-distribution (OOD) graph classification tasks based on our Structural Causal Model (SCM) (described in Definitions 1 and 2 and Figure 1), the possible solution to solve this extrapolation problem and an environment-invariant graph representation that is able to extrapolate to OOD test data.

The shortcomings of standard graph representation methods. Figure 1 shows that our target variable Y is a function only of the *graphon* variable W , rather than the training or test environments, E^{tr} and E^{te} , respectively. However, due to the reverse (backdoor) path between Y and E^{tr} through N^{tr} and X^{tr} in the DAG, Y is not independent of E^{tr} given $\mathcal{G}_{N^{\text{tr}}}^{\text{te}}$. Hence, traditional graph representation learning methods can pick-up this correlation in the training data, which would prevent the model learning the correct OOD test predictor $P(Y | \mathcal{G}_{N^{\text{te}}}^{\text{te}})$ [7, 112, 33].

To address the challenge of correctly predicting Y in our OOD test data, regardless of backdoor paths, we need an estimator that can account for it. In our SCM, we can apply Pearl’s backdoor adjustment [97, Theorem 3.3.2]:

$$P(Y | \mathcal{G}_{N^{\text{te}}}^{\text{te}}) = \sum_{e^{\dagger} \in \text{supp}(E^{\text{te}})} P(Y | \mathcal{G}_{N^{\text{tr}}}^{\text{tr}}, E^{\text{tr}} = e^{\dagger}) P(E^{\text{te}} = e^{\dagger}). \quad (2)$$

There are, however, two big challenges to applying Equation (2): (a) We do not know $P(E^{\text{te}} = e)$ and, most importantly, (b) the test support may not be a subset of the train support, i.e., $\text{supp}(E^{\text{te}}) \not\subseteq \text{supp}(E^{\text{tr}})$.

Hence, in what follows we focus on **environment-invariant (E-invariant)** graph representations $\Gamma(\cdot)$, such that $\forall e \in \text{supp}(E^{\text{tr}}), \forall e^\dagger \in \text{supp}(E^{\text{te}})$,

$$\mathbb{P}(Y|\Gamma(\mathcal{G}_{N^{\text{tr}}}^{\text{tr}}), E^{\text{tr}} = e) = \mathbb{P}(Y|\Gamma(\mathcal{G}_{N^{\text{te}}}^{\text{te}}), E^{\text{te}} = e^\dagger),$$

which eliminates the need for conditioning on the environments in Equation (2). For this, we first introduce the effect of E-invariant representations on downstream classification tasks.

Proposition 1. *[E-invariant Representation's Effect on Classification] Consider a permutation-invariant graph representation $\Gamma : \cup_{n=1}^{\infty} \{0, 1\}^{n \times n} \times \mathbb{X}^n \rightarrow \mathbb{R}^d$, $d \geq 1$, and a downstream function $\rho : \mathbb{Y} \times \mathbb{R}^d \rightarrow [0, 1]$ (e.g., a feedforward neural network (MLP) with softmax outputs) such that, for some $\epsilon, \delta > 0$, the generalization error over the training distribution is: For $\forall y \in \mathbb{Y}$,*

$$\mathbb{P}(|\mathbb{P}(Y = y|\mathcal{G}_{N^{\text{tr}}}^{\text{tr}}) - \rho(y, \Gamma(\mathcal{G}_{N^{\text{tr}}}^{\text{tr}}))| \leq \epsilon) \geq 1 - \delta,$$

Γ is said to be **environment-invariant (E-invariant)** if $\forall e \in \text{supp}(E^{\text{tr}}), \forall e^\dagger \in \text{supp}(E^{\text{te}})$,

$$\Gamma(\mathcal{G}_{N^{\text{tr}}}^{\text{tr}}|E^{\text{tr}} = e) = \Gamma(\mathcal{G}_{N^{\text{te}}}^{\text{te}}|E^{\text{te}} = e^\dagger).$$

Then, the OOD test error is the same as the generalization error over the training distribution, i.e., for $\forall y \in \mathbb{Y}$,

$$\mathbb{P}(|\mathbb{P}(Y = y|\mathcal{G}_{N^{\text{te}}}^{\text{te}}) - \rho(y, \Gamma(\mathcal{G}_{N^{\text{te}}}^{\text{te}}))| \leq \epsilon) \geq 1 - \delta. \quad (3)$$

Proposition 1 shows that an E-invariant representation will perform no worse on the OOD test data (extrapolation samples from $(Y, \mathcal{G}_{N^{\text{te}}}^{\text{te}})$) than on a test dataset having the same environment distribution as the training data (samples from $(Y, \mathcal{G}_{N^{\text{tr}}}^{\text{tr}})$). Our task now becomes finding an E-invariant graph representation Γ that can be used to predict Y .

The shortcomings of Invariant Risk Minimization (IRM). Invariant Risk Minimization (IRM) [7] aims to learn a representation that is invariant across all training environment, $\forall e \in \text{supp}(E^{\text{tr}})$, by adding a regularization penalty on the empirical risk. However, IRM will fail if: (i) $\text{supp}(E^{\text{te}}) \not\subseteq \text{supp}(E^{\text{tr}})$, since the penalty provides no guarantee that the representation will still be invariant w.r.t. $e^\dagger \in \text{supp}(E^{\text{te}}) \setminus \text{supp}(E^{\text{tr}})$; and (ii) if the training data only contains a single environment, i.e., $\text{supp}(E^{\text{tr}}) = \{e\}$. For instance, the training data may contain only graphs of a single size. In this case, we are unable to apply IRM for size extrapolations. Our experiments show that the IRM procedure of Arjovsky et al. [7] does not seem to work for graph representation learning.

In what follows we leverage the stability of subgraph densities (more precisely, induced homomorphism densities) in graphon random graph models [79] to learn E-invariant representations for the SCM defined in Definitions 1 and 2, whose DAG is illustrated in Figure 1.

3.1 An Approximately E-Invariant Graph Representations for Our Model

Let $\mathcal{G}_{N^*}^*$ denote either an N^{tr} -sized train or N^{te} -sized test graph from the SCM in Definitions 1 and 2. For a given k -vertex graph F_k ($k < N^*$), let $\text{ind}(F_k, \mathcal{G}_{N^*}^*)$ be the number of induced homomorphisms of F_k into $\mathcal{G}_{N^*}^*$, informally, the number of mappings from $V(F_k)$ to $V(\mathcal{G}_{N^*}^*)$ such that the corresponding subgraph induced in $\mathcal{G}_{N^*}^*$ is isomorphic to F_k . The induced homomorphism density is defined as

$$t_{\text{ind}}(F_k, \mathcal{G}_{N^*}^*) = \frac{\text{ind}(F_k, \mathcal{G}_{N^*}^*)}{N^*!/(N^* - k)!}, \quad (4)$$

where the denominator is the number of possible mappings. Let $\mathcal{F}_{\leq k}$ be the set of all connected vertex-attributed graphs of size $k' \leq k$. Using the subgraph densities (induced homomorphism densities) $\{t_{\text{ind}}(F_{k'}, \mathcal{G}_{N^*}^*)\}_{F_{k'} \in \mathcal{F}_{\leq k}}$ we will construct a (feature vector) representation for $\mathcal{G}_{N^*}^*$, similar to Hancock and Khoshgoftaar [52], Pinar et al. [100],

$$\Gamma_{\text{1-hot}}(\mathcal{G}_{N^*}^*) = \sum_{F_{k'} \in \mathcal{F}_{\leq k}} t_{\text{ind}}(F_{k'}, \mathcal{G}_{N^*}^*) \mathbf{1}_{\text{one-hot}}\{F_{k'}, \mathcal{F}_{\leq k}\}, \quad (5)$$

where $\mathbf{1}_{\text{one-hot}}\{F_{k'}, \mathcal{F}_{\leq k}\}$ assigns a unique one-hot vector to each distinct graph $F_{k'}$ in $\mathcal{F}_{\leq k}$. For instance, for $k = 4$, the one-hot vectors could be $(1, 0, \dots, 0) = \textcolor{red}{\bullet}$, $(0, 1, \dots, 0) = \textcolor{blue}{\bullet}$, $(0, 0, \dots, 1, \dots, 0) = \textcolor{red}{\bullet}$, $(0, 0, \dots, 1) = \textcolor{blue}{\bullet}$, etc.. In Section 3.2 we show that the (feature vector) representation in Equation (5) is approximately environment-invariant in our SCM model.

An alternative approach is to replace the one-hot vector representation with learnable graph representation models. We first use Graph Neural Networks (GNNs) [65, 50, 147] to learn representations that can capture information from vertex attributes. Simply speaking, GNNs proceed by vertices passing messages, amongst each other, through a learnable function such as an MLP, and repeating $L \in \mathbb{Z}_{\geq 1}$ layers.

Consider the following simple GNN example. Let V^* be the set of vertices. At each iteration $l \in \{1, 2, \dots, L\}$, all vertices $v \in V^*$ are associated with a learned vector $\mathbf{h}_v^{(l)}$. Specifically, we begin by initializing a vector as $\mathbf{h}_v^{(0)} = X_v$ for every vertex $v \in V^*$. Then, we recursively compute an update such as the following $\forall v \in V^*$,

$$\mathbf{h}_v^{(l)} = \text{MLP}^{(l)}\left(\mathbf{h}_v^{(l-1)}, \text{READOUT}_{\text{Neigh}}((\mathbf{h}_u^{(l-1)})_{u \in \mathcal{N}(v)})\right), \quad (6)$$

where $\mathcal{N}(v) \subseteq V^*$ denotes the neighborhood set of v in the graph, $\text{READOUT}_{\text{Neigh}}$ is a permutation-invariant function (e.g. sum) of the neighborhood learned vectors, $\text{MLP}^{(l)}$ denotes a multi-layer perceptron and whose superscript l indicates that the MLP at each recursion layer may have different learnable parameters. There are other alternatives to Equation (6) that we will also test in our experiments.

Then, we arrive to the following representation of $\mathcal{G}_{N^*}^*$:

$$\Gamma_{\text{GNN}}(\mathcal{G}_{N^*}^*) = \sum_{F_{k'} \in \mathcal{F}_{\leq k}} t_{\text{ind}}(F_{k'}, \mathcal{G}_{N^*}^*) \text{READOUT}_{\Gamma}(\text{GNN}(F_{k'})), \quad (7)$$

where READOUT_{Γ} is a permutation-invariant function that maps the vertex-level outputs of a GNN to a graph-level representation (e.g. by summing all vertex embeddings). Unfortunately, GNNs are not most-expressive representations of graphs [86, 89, 142] and thus $\Gamma_{\text{GNN}}(\cdot)$ is less expressive than $\Gamma_{\text{1-hot}}(\cdot)$ in generalization over the training distribution. A representation with greater expressiveness power is

$$\Gamma_{\text{GNN}^+}(\mathcal{G}_{N^*}^*) = \sum_{F_{k'} \in \mathcal{F}_{\leq k}} t_{\text{ind}}(F_{k'}, \mathcal{G}_{N^*}^*) \text{READOUT}_{\Gamma}(\text{GNN}^+(F_{k'})), \quad (8)$$

where GNN^+ is a most-expressive k' -vertex graph representation, which can be achieved by any of the methods of Vignac et al. [134], Maron et al. [81], Murphy et al. [89]. Since GNN^+ is most expressive, GNN^+ can ignore attributes and map each $F_{k'}$ to a one-hot vector $\mathbf{1}_{\text{one-hot}}\{F_{k'}, \mathcal{F}_{\leq k}\}$; therefore, $\Gamma_{\text{GNN}^+}(\cdot)$ generalizes $\Gamma_{\text{1-hot}}(\cdot)$ of Equation (5). But **note** that greater expressiveness does not imply better extrapolation.

More importantly, GNN and GNN^+ representations allow us to increase their E-invariance by adding a penalty for having different representations of two graphs $F_{k'}$ and $H_{k'}$ with the same topology but different vertex attributes (say, $F_{k'} = \text{graph with red and blue nodes}$ and $H_{k'} = \text{graph with red and green nodes}$), as long as these differences do not significantly impact downstream model accuracy in the training data. We will discuss more about the theoretical underpinnings in the next section. Hence, for each k' -sized vertex-attributed graph $F_{k'}$, we consider the set $\mathcal{H}(F_{k'})$ of all k' -sized vertex-attributed graphs having the same underlying topology as $F_{k'}$ but with all possible different vertex attributes. We then define the regularization penalty

$$\frac{1}{|\mathcal{F}_{\leq k}|} \sum_{F_{k'} \in \mathcal{F}_{\leq k}} \mathbb{E}_{H_{k'} \in \mathcal{H}(F_{k'})} \|\text{READOUT}_{\Gamma}(\text{GNN}^*(F_{k'})) - \text{READOUT}_{\Gamma}(\text{GNN}^*(H_{k'}))\|_2, \quad (9)$$

where $\text{GNN}^* = \text{GNN}$ if we choose the representation Γ_{GNN} , or $\text{GNN}^* = \text{GNN}^+$ if we choose the representation Γ_{GNN^+} . In practice, we assume $H_{k'}$ is uniformly sampled from $\mathcal{H}(F_{k'})$ and we sample one $H_{k'}$ for each $F_{k'}$ in order to obtain an unbiased estimator of Equation (9).

Practical considerations. Efficient algorithms exist to obtain *induced* homomorphism densities over all possible *connected* k -vertex subgraphs [2, 23, 27, 28, 106, 137]. For unattributed graphs and $k \leq 5$, we use ESCAPE [100] to obtain *exact* densities. For attributed graphs or unattributed graphs with $k > 5$, exact counting becomes intractable, so we use R-GPM [126] to obtain unbiased estimates of densities. Finally, Proposition 2 in Appendix C shows that certain biased estimators can be used if READOUT_{Γ} is the sum of vertex embeddings.

3.2 Theoretical Description of our E-Invariant Graph Representations

In this section, we show that the graph representations seen in the previous section are approximately environment-invariant in our SCM model under slight assumptions.

Theorem 1 (Approximate E-invariant Graph Representation). *Let $\mathcal{G}_{N^{\text{tr}}}^{\text{tr}}$ and $\mathcal{G}_{N^{\text{te}}}^{\text{te}}$ be two samples of graphs of sizes N^{tr} and N^{te} from the training and test distributions, respectively, both defined over the same graphon variable W and satisfying Definitions 1 and 2. Assume the vertex attribute function $g_X(\cdot)$ of Definitions 1 and 2 is invariant to E^{tr} and E^{te} (the reason for this assumption will be clear later). Let $\|\cdot\|_{\infty}$ denotes the L-infinity norm. For any integer $k \leq \min(N^{\text{tr}}, N^{\text{te}})$, and any constant $0 < \epsilon < 1$,*

$$\mathbb{P}(\|\Gamma_{\text{1-hot}}(\mathcal{G}_{N^{\text{tr}}}^{\text{tr}}) - \Gamma_{\text{1-hot}}(\mathcal{G}_{N^{\text{te}}}^{\text{te}})\|_{\infty} > \epsilon) \leq 2|\mathcal{F}_{\leq k}| \left(\exp\left(-\frac{\epsilon^2 N^{\text{tr}}}{8k^2}\right) + \exp\left(-\frac{\epsilon^2 N^{\text{te}}}{8k^2}\right) \right). \quad (10)$$

Theorem 1 shows how the graph representations given in Equation (5) are approximately E-invariant. Note that for unattributed graphs, we can define $g_X(\cdot, \cdot) = \cdot$ as the null attribute, which is invariant to any environment by construction. For graphs with attributed vertices, $g_X(\cdot, \cdot)$ being invariant to E^{tr} and E^{te} means for any two environment $e \in \text{supp}(E^{\text{tr}}), e^\dagger \in \text{supp}(E^{\text{te}}), g_X(e, \cdot) = g_X(e^\dagger, \cdot)$.

Theorem 1 shows that for $k \ll \min(N^{\text{tr}}, N^{\text{te}})$, the representations $\Gamma_{1\text{-hot}}(\cdot)$ of two possibly different-sized graphs with the same W are nearly identical, indicating $\Gamma_{1\text{-hot}}(\mathcal{G}_{N^*}^*)$ is an approximately E-invariant representation.

Theorem 1 also exposes a trade-off, however. If the observed graphs tend to be relatively small, the required k for approximately E-invariant representations can be small, and then the expressiveness of $\Gamma_{1\text{-hot}}(\cdot)$ gets compromised. That is, the ability of $\Gamma_{1\text{-hot}}(\mathcal{G}_{N^*}^*)$ to extract information about W from $\mathcal{G}_{N^*}^*$ reduces as k decreases. Finally, this guarantees that for appropriate k , passing the representation $\Gamma_{1\text{-hot}}(\mathcal{G}_{N^*}^*)$ to a downstream classifier provably approximates the classifier in Equation (3) of Proposition 1.

Note that when the vertex attributes are not invariant to the environment variable, $\Gamma_{1\text{-hot}}(\cdot)$ is not E-invariant and we can not extrapolate using $\Gamma_{1\text{-hot}}(\cdot)$. Thankfully, for the GNN-based graph representations $\Gamma_{\text{GNN}}(\mathcal{G}_{N^*}^*)$ and $\Gamma_{\text{GNN+}}(\mathcal{G}_{N^*}^*)$ in Equations (7) and (8), respectively, the regularization penalty in Equation (9) pushes the representation of vertex attributes to be more E-invariant, making it more likely to satisfy the conditions of E-invariance in Theorem 1. In particular, consider the attributed SBM example in Section 2, the environment operates on changing the distributions of attributes assigned in each block. If we are going to predict cross-block edge probabilities (see Section 5.2), we need the representations to merge attributes that are assigned to the same block to achieve E-invariance. By regularizing the GNN-based graph representation towards merging the representations of different vertex attributes, we can get an approximately E-invariant representation in this setting.

4 Related Work

This section presents an overview of the related work. Due to space constraints, a more in-depth discussion with further references is given in Appendix E. In particular, Appendix E gives a detailed description of environment-invariant methods that require multiple environments in training, including *Independence of Causal Mechanism (ICM)*, *Causal Discovery from Change (CDC)*, and *representation disentanglement* methods. None of these works focus on graphs.

OOD extrapolation in graph classification and size extrapolation in GNNs. Our work ascertain a causal relationship between graphs and their target labels. We are unaware of existing work on this topic. Xu et al. [143] is interested on a geometric (non-causal) definition of extrapolation for a class of graph algorithms. Hu et al. [57] introduces a large graph dataset presenting significant challenges of OOD extrapolation, however, their shift is on the two-dimensional structural framework distribution of the molecules, and no causal model is provided. The parallel work of Yehudai et al. [146] improves size extrapolation in GNNs using self-supervised and semi-supervised learning on both the training and test domain, which is orthogonal to our problem. Previous works also examine empirically the ability of graph neural networks to extrapolate in various applications, such as physics [13, 108], mathematical and abstract reasoning [109, 111], and graph algorithms [16, 92, 14, 59, 133]. These works do not provide guarantees of test extrapolation performance, a causal model, or a proof that the tasks require extrapolation over different environments.

Graph classification using induced homomorphisms. A related set of works look at induced homomorphism densities as graph features for a kernel [116, 144, 135]. These methods can perform poorly in some tasks [69]. Recent work has also shown an interest in induced subgraphs, which are used to improve predictions of GNNs [22] or as input for newly-proposed architectures [129]. None of these methods focus on invariant representations or extrapolations.

Expressiveness of graph representations. The expressiveness of a graph representation method is a measure of model family bias [86, 142, 41, 81, 89]. That is, given enough training data, a neural network from a more expressive family can achieve smaller generalization error over the training distribution than a neural network from a less expressive family, assuming appropriate optimization. However, this power is a measure of generalization capability over the training distribution, not OOD extrapolation. Hence, the question of representation expressiveness is orthogonal to our work.

5 Empirical Results

This section is dedicated to the empirical evaluation of our theoretical claims, including the ability of the representations in Equations (5), (7) and (8) to extrapolate as predicted by Proposition 1 for tasks that abide by Definitions 1 and 2. Due

Table 1: Extrapolation performance over *unattributed* graphs **shows clear advantage of our environment-invariant representations, with or without GNN, over standard methods or IRM in extrapolation test accuracy**. Table shows mean (standard deviation) accuracy. Bold emphasises the best test average. NA value indicates IRM is not applicable (when training data has a single graph size).

ACCURACY IN SCHIZOPHRENIA TASK			ACCURACY IN ERDŐS-RÉNYI TASK					
TRAINING HAS A SINGLE GRAPH SIZE			TRAINING HAS A SINGLE GRAPH SIZE			TRAINING HAS TWO GRAPH SIZES		
TRAIN [$P(Y, G_{N^{\text{tr}}}^{\text{te}})$]	VAL. [$P(Y, G_{N^{\text{tr}}}^{\text{te}})$]	TEST (\uparrow) [$P(Y, G_{N^{\text{tr}}}^{\text{te}})$]	TRAIN [$P(Y, G_{N^{\text{tr}}}^{\text{te}})$]	VAL. [$P(Y, G_{N^{\text{tr}}}^{\text{te}})$]	TEST (\uparrow) [$P(Y, G_{N^{\text{tr}}}^{\text{te}})$]	TRAIN [$P(Y, G_{N^{\text{tr}}}^{\text{te}})$]	VAL. [$P(Y, G_{N^{\text{tr}}}^{\text{te}})$]	TEST (\uparrow) [$P(Y, G_{N^{\text{tr}}}^{\text{te}})$]
PNA	0.99 (0.00)	0.76 (0.08)	0.61 (0.08)	1.00 (0.00)	1.00 (0.00)	0.65 (0.12)	1.00 (0.00)	1.00 (0.00) 0.64 (0.12)
PNA (MEAN XU-READOUT)	0.99 (0.00)	0.77 (0.07)	0.53 (0.10)	1.00 (0.00)	1.00 (0.00)	0.62 (0.12)	1.00 (0.00)	1.00 (0.00) 0.51 (0.19)
PNA (MAX XU-READOUT)	0.99 (0.00)	0.75 (0.07)	0.42 (0.06)	1.00 (0.00)	1.00 (0.00)	0.59 (0.16)	0.99 (0.01)	1.00 (0.00) 0.57 (0.15)
PNA + IRM	NA	NA	NA	NA	NA	NA	1.00 (0.00)	1.00 (0.00) 0.65 (0.13)
GCN	0.74 (0.04)	0.74 (0.08)	0.55 (0.09)	0.99 (0.01)	1.00 (0.00)	0.88 (0.10)	0.98 (0.01)	1.00 (0.00) 0.87 (0.10)
GCN (MEAN XU-READOUT)	0.72 (0.04)	0.73 (0.08)	0.65 (0.08)	0.99 (0.01)	1.00 (0.00)	0.79 (0.15)	0.98 (0.02)	1.00 (0.00) 0.75 (0.20)
GCN (MAX XU-READOUT)	0.86 (0.07)	0.75 (0.07)	0.54 (0.06)	0.99 (0.01)	1.00 (0.00)	0.90 (0.07)	0.96 (0.04)	1.00 (0.00) 0.87 (0.09)
GCN + IRM	NA	NA	NA	NA	NA	NA	0.98 (0.02)	1.00 (0.00) 0.88 (0.08)
GIN	0.72 (0.02)	0.74 (0.05)	0.36 (0.09)	1.00 (0.00)	1.00 (0.00)	0.64 (0.12)	1.00 (0.00)	1.00 (0.00) 0.65 (0.12)
GIN (MEAN XU-READOUT)	0.78 (0.02)	0.72 (0.05)	0.43 (0.05)	1.00 (0.00)	1.00 (0.00)	0.63 (0.09)	1.00 (0.00)	1.00 (0.00) 0.61 (0.09)
GIN (MAX XU-READOUT)	0.85 (0.02)	0.72 (0.05)	0.35 (0.06)	0.99 (0.01)	1.00 (0.00)	0.65 (0.12)	1.00 (0.00)	1.00 (0.00) 0.65 (0.07)
GIN + IRM	NA	NA	NA	NA	NA	NA	1.00 (0.00)	1.00 (0.00) 0.66 (0.08)
RPGIN	0.70 (0.02)	0.74 (0.05)	0.37 (0.06)	1.00 (0.00)	1.00 (0.00)	0.61 (0.16)	1.00 (0.00)	1.00 (0.00) 0.60 (0.16)
WL KERNEL	1.00 (0.00)	0.63 (0.07)	0.40 (0.06)	1.00 (0.00)	1.00 (0.00)	0.51 (0.00)	1.00 (0.00)	1.00 (0.00) 0.30 (0.00)
GC KERNEL	0.61 (0.00)	0.61 (0.06)	0.60 (0.00)	1.00 (0.00)	1.00 (0.00)	1.00 (0.00)	1.00 (0.00)	1.00 (0.00) 1.00 (0.00)
$\Gamma_{\text{1-HOT}}$	0.71 (0.01)	0.72 (0.05)	0.72 (0.04)	1.00 (0.00)	1.00 (0.00)	1.00 (0.00)	1.00 (0.00)	1.00 (0.00) 1.00 (0.00)
Γ_{GIN}	0.75 (0.05)	0.70 (0.04)	0.68 (0.07)	1.00 (0.00)	1.00 (0.00)	1.00 (0.00)	1.00 (0.00)	1.00 (0.00) 1.00 (0.00)
Γ_{RPGIN}	0.69 (0.01)	0.71 (0.06)	0.71 (0.03)	1.00 (0.00)	1.00 (0.00)	1.00 (0.00)	1.00 (0.00)	1.00 (0.00) 1.00 (0.00)

Table 2: Extrapolation performance over *attributed* graphs **shows clear advantage of environment-invariant representations with GNNs and the attribute regularization in Equation (9)**. Table shows mean (standard deviation) accuracy. Bold emphasises the best test average. NA value indicates IRM is not applicable (when training data has a single graph size).

TRAINING HAS A SINGLE GRAPH SIZE 20			TRAINING HAS TWO GRAPH SIZES: 14 AND 20			TRAINING HAS TWO GRAPH SIZES: 20 AND 30		
TRAIN [$P(Y, G_{N^{\text{tr}}}^{\text{te}})$]	VAL. [$P(Y, G_{N^{\text{tr}}}^{\text{te}})$]	TEST (\uparrow) [$P(Y, G_{N^{\text{tr}}}^{\text{te}})$]	TRAIN [$P(Y, G_{N^{\text{tr}}}^{\text{te}})$]	VAL. [$P(Y, G_{N^{\text{tr}}}^{\text{te}})$]	TEST (\uparrow) [$P(Y, G_{N^{\text{tr}}}^{\text{te}})$]	TRAIN [$P(Y, G_{N^{\text{tr}}}^{\text{te}})$]	VAL. [$P(Y, G_{N^{\text{tr}}}^{\text{te}})$]	TEST (\uparrow) [$P(Y, G_{N^{\text{tr}}}^{\text{te}})$]
PNA	1.00 (0.00)	1.00 (0.00)	0.65 (0.10)	0.96 (0.06)	0.94 (0.03)	0.57 (0.19)	0.99 (0.01)	1.00 (0.00) 0.69 (0.19)
PNA (MEAN XU-READOUT)	1.00 (0.00)	1.00 (0.00)	0.86 (0.13)	0.97 (0.02)	0.95 (0.02)	0.64 (0.11)	0.99 (0.01)	1.00 (0.00) 0.70 (0.15)
PNA (MAX XU-READOUT)	0.99 (0.01)	0.97 (0.02)	0.83 (0.13)	0.94 (0.04)	0.93 (0.03)	0.80 (0.12)	0.95 (0.05)	0.95 (0.05) 0.80 (0.15)
PNA + IRM	NA	NA	NA	0.95 (0.05)	0.94 (0.03)	0.58 (0.19)	0.99 (0.01)	1.00 (0.00) 0.70 (0.20)
GCN	0.99 (0.01)	0.98 (0.02)	0.62 (0.09)	0.95 (0.02)	0.96 (0.02)	0.55 (0.17)	1.00 (0.00)	1.00 (0.00) 0.73 (0.17)
GCN (MEAN XU-READOUT)	0.94 (0.03)	0.99 (0.01)	0.61 (0.12)	0.93 (0.05)	0.94 (0.02)	0.69 (0.20)	1.00 (0.00)	1.00 (0.00) 0.84 (0.13)
GCN (MAX XU-READOUT)	0.99 (0.01)	1.00 (0.00)	0.76 (0.07)	0.95 (0.04)	0.98 (0.02)	0.61 (0.17)	0.98 (0.02)	1.00 (0.00) 0.70 (0.20)
GCN + IRM	NA	NA	NA	0.93 (0.05)	0.97 (0.03)	0.65 (0.19)	1.00 (0.00)	1.00 (0.00) 0.84 (0.17)
GIN	0.97 (0.02)	1.00 (0.00)	0.64 (0.17)	0.95 (0.03)	0.96 (0.04)	0.66 (0.20)	0.98 (0.02)	1.00 (0.00) 0.74 (0.19)
GIN (MEAN XU-READOUT)	1.00 (0.00)	1.00 (0.00)	0.85 (0.14)	0.97 (0.01)	0.99 (0.01)	0.75 (0.18)	0.99 (0.01)	1.00 (0.00) 0.80 (0.15)
GIN (MAX XU-READOUT)	0.95 (0.02)	0.97 (0.03)	0.67 (0.18)	0.93 (0.06)	0.94 (0.03)	0.67 (0.17)	0.99 (0.01)	1.00 (0.00) 0.69 (0.15)
GIN + IRM	NA	NA	NA	0.95 (0.03)	0.97 (0.04)	0.64 (0.19)	0.98 (0.02)	1.00 (0.00) 0.75 (0.19)
RPGIN	0.98 (0.02)	1.00 (0.00)	0.49 (0.16)	0.96 (0.03)	0.99 (0.01)	0.54 (0.12)	0.99 (0.01)	1.00 (0.00) 0.50 (0.13)
WL KERNEL	1.00 (0.00)	0.95 (0.00)	0.57 (0.00)	0.99 (0.00)	0.90 (0.00)	0.62 (0.00)	1.00 (0.00)	1.00 (0.00) 0.57 (0.00)
GC KERNEL	1.00 (0.00)	0.90 (0.00)	0.43 (0.00)	1.00 (0.00)	0.80 (0.00)	0.43 (0.00)	0.99 (0.00)	0.90 (0.00) 0.43 (0.00)
$\Gamma_{\text{1-HOT}}$	1.00 (0.00)	0.90 (0.00)	0.50 (0.07)	0.97 (0.03)	0.85 (0.05)	0.50 (0.07)	0.98 (0.00)	0.96 (0.02) 0.45 (0.05)
Γ_{GIN}	1.00 (0.00)	1.00 (0.00)	0.98 (0.02)	0.96 (0.02)	0.95 (0.01)	0.95 (0.06)	1.00 (0.00)	1.00 (0.00) 0.88 (0.12)
Γ_{RPGIN}	1.00 (0.00)	1.00 (0.00)	1.00 (0.00)	0.97 (0.03)	0.95 (0.02)	0.95 (0.05)	1.00 (0.00)	1.00 (0.00) 0.93 (0.05)

to space constraints, our results are summarised here, while further details are relegated to Appendix F. Our code is available¹.

We explore the extrapolation power of $\Gamma_{\text{1-HOT}}$, Γ_{GIN} and Γ_{RPGIN} of Equations (5), (7) and (8) using the Graph Isomorphism Network (GIN) [142] as our base GNN model, and Relational Pooling GIN (RPGIN) [89] as a more expressive GNN. The graph representations are then passed to a L -hidden layer feedforward neural network (MLP) with softmax outputs that give the predicted classes, $L \in \{0, 1\}$. As described in Section 3.1, we obtain induced homomorphism densities of connected graphs. For practical reasons, we focus only on densities of graphs of size *exactly* k , which is treated as a hyperparameter.

Baselines. Our baselines include the Graphlet Counting kernel (GC Kernel) [116], which uses the $\Gamma_{\text{1-HOT}}$ representation as input to a downstream classifier. We report $\Gamma_{\text{1-HOT}}$ separately from GC Kernel since $\Gamma_{\text{1-HOT}}$ differs from GC Kernel in that we add the same feedforward neural network (MLP) classifier used in the Γ_{GIN} model. We also include GIN [142], GCN [65] and PNA [30], considering the sum, mean, and max READOUTs as proposed by Xu et al. [143] for extrapolations (which we denote as *XU-READOUT* to not confuse with our READOUT_{Γ}). We also examine a more-expressive GNN, RPGIN [89], and the WL Kernel [117]. We do not use the method of Yehudai et al. [146] as a baseline since it is a covariate shift adaptation approach that requires samples from $\mathcal{P}(\mathcal{G}_{N^{\text{tr}}}^{\text{te}})$, which are not available in our setting.

Experiments with single and multiple graph sizes in training. Our single-environment experiments consist of a single graph size in training, and different sizes in test (different from the training size). Whenever multiple environments are available in training —multiple environments implies different graph sizes—, we employ Invariant Risk Minimization (IRM), considering the penalty proposed by Arjovsky et al. [7] for each environment (defined empirically as a range of training examples with similar graph sizes).

For each task, we report (a) *training* accuracy (b) *validation* accuracy, which are new examples sampled from $\mathcal{P}(Y, \mathcal{G}_{N^{\text{tr}}}^{\text{tr}})$; and (c) *extrapolation test* accuracy, which are new OOD examples sampled from $\mathcal{P}(Y, \mathcal{G}_{N^{\text{te}}}^{\text{te}})$. In our experiments we perform early stopping as per Hu et al. [57].

¹<https://github.com/PurdueMINDS/size-invariant-GNNs>

Table 3: Extrapolation performance over real-world graph datasets with OOD tasks violating Definitions 1 and 2 and conditions of Theorem 1. Always one of our E-invariant representations Γ_{GIN} and Γ_{RPGIN} is amongst the top 4 best methods in all datasets except NCI109. Table shows mean (standard deviation) Matthews correlation coefficient (MCC) of the classifiers over the OOD test data. Bold emphasises the top-4 models (in average MCC) for each dataset.

DATASETS	NCI1	NCI109	PROTEINS	DD
RANDOM	0.00 (0.00)	0.00 (0.00)	0.00 (0.00)	0.00 (0.00)
PNA	0.21 (0.06)	0.24 (0.06)	0.26 (0.08)	0.24 (0.10)
PNA MEAN (XU-READOUT)	0.12 (0.05)	0.21 (0.04)	0.25 (0.06)	0.29 (0.08)
PNA MAX (XU-READOUT)	0.16 (0.05)	0.18 (0.07)	0.20 (0.05)	0.12 (0.14)
PNA + IRM	0.21 (0.07)	0.27 (0.08)	0.26 (0.10)	0.26 (0.08)
GCN	0.20 (0.06)	0.15 (0.06)	0.21 (0.09)	0.23 (0.05)
GCN MEAN (XU-READOUT)	0.20 (0.04)	0.15 (0.09)	0.23 (0.07)	0.19 (0.06)
GCN MAX (XU-READOUT)	0.20 (0.04)	0.19 (0.07)	0.20 (0.14)	0.09 (0.08)
GCN + IRM	0.12 (0.05)	0.22 (0.06)	0.20 (0.07)	0.23 (0.07)
GIN	0.25 (0.06)	0.18 (0.05)	0.23 (0.05)	0.25 (0.09)
GIN MEAN (XU-READOUT)	0.16 (0.05)	0.14 (0.05)	0.24 (0.05)	0.27 (0.12)
GIN MAX (XU-READOUT)	0.15 (0.08)	0.18 (0.08)	0.28 (0.11)	0.19 (0.07)
GIN + IRM	0.18 (0.08)	0.16 (0.04)	0.26 (0.06)	0.21 (0.09)
RPGIN	0.15 (0.04)	0.19 (0.05)	0.24 (0.09)	0.22 (0.09)
WL KERNEL	0.39 (0.00)	0.21 (0.00)	0.00 (0.00)	0.00 (0.00)
GC KERNEL	0.02 (0.00)	0.01 (0.00)	0.29 (0.00)	0.00 (0.00)
$\Gamma_{1\text{-HOT}}$	0.17 (0.08)	0.25 (0.06)	0.12 (0.09)	0.23 (0.08)
Γ_{GIN}	0.24 (0.04)	0.18 (0.04)	0.29 (0.11)	0.28 (0.06)
Γ_{RPGIN}	0.26 (0.05)	0.20 (0.04)	0.25 (0.12)	0.20 (0.05)

5.1 Size extrapolation tasks for unattributed graphs

Schizophrenia task. We use the fMRI brain graph data on 71 schizophrenic patients and 74 controls for classifying individuals with schizophrenia [32]. Vertices represent brain regions (voxels) with edges as functional connectivity. We process the graph differently between training and test data, where training graphs have exactly 264 vertices (a single environment) and control-group graphs in test have around 40% fewer vertices. We employ a 5-fold cross-validation for hyperparameter tuning.

Erdős-Rényi task. We simulate Erdős-Rényi graphs [42, 38] as a simple graphon random graph model. The task is to classify the edge probability $p \in \{0.2, 0.5, 0.8\}$ of the generated graph. First we consider a single-environment version of the task, where we train and validate on graphs of size 80 and extrapolate to graphs with size 140 in test. We also consider another experiment with training/validation graph sizes uniformly selected from $\{70, 80\}$ (so we can use IRM), with the test data same as before (graphs of size 140 in test).

Results. Table 1 shows that all methods perform well in validation (generalization over the training distribution). However, only $\Gamma_{1\text{-hot}}$ (GC Kernel and our simple classifier), Γ_{GIN} , Γ_{RPGIN} are able to extrapolate, while displaying very similar—often identical—accuracies in validation (sampled from $P(\mathcal{G}_{N^{\text{tr}}}^{\text{tr}})$) and test (sampled from $P(\mathcal{G}_{N^{\text{te}}}^{\text{te}})$) in all experiments, as predicted by combining the theoretical results in Proposition 1 and Theorem 1. Using IRM in the Erdős-Rényi task shows no improvement over not using IRM in the multi-environment setting.

5.2 Size/attribute extrapolation for attributed graphs

We now define a Stochastic Block Model (SBM) task with vertex attributes. The SBM has two blocks. Our goal is to classify the cross-block edge probability $P_{1,2} = P_{2,1} \in \{0.1, 0.3\}$ of a sampled graph. Vertex attribute distributions depend on the blocks. In block 1 vertices are randomly assigned red and blue attributes, while in block 2 vertices are randomly assigned green and yellow attributes (see **SBM with vertex attributes** in Section 2).

The change in environments between training and test introduces a joint attribute-and-size distribution shift: In training, the vertices are 90% red (resp. green) and 10% blue (resp. yellow) in block 1 (resp. block 2). While in test, the distribution is flipped and vertices are 10% red (resp. green) and 90% blue (resp. yellow) in block 1 (resp. block 2). We consider three scenarios, with the same test data made of graphs of size 40: (a) A single-environment case, where all training graphs have size 20; (b) A multi-environment case, where training graphs have sizes 14 and 20; (c) A multi-environment case, where training graphs have sizes 20 and 30. These differences in training data will check whether having graphs of sizes closer to the test graph sizes improves the performance of traditional graph representation methods.

Results. Table 2 shows how traditional graph representations and $\Gamma_{1\text{-hot}}$ (both GC Kernel and our neural classifier) taps into the easy correlation between Y and the density of red and green vertex attributes in the training graphs, while Γ_{GIN} and Γ_{RPGIN} , with their attribute regularization (Equation (9)), are approximately E-invariant, resulting in higher test accuracy that more closely matches their validation accuracy. Moreover, applying IRM has no beneficial impact, while adding larger graphs in training (closer to test graph sizes) increases the extrapolation accuracy of most methods.

5.3 Experiments with real-world datasets that violate our causal model

Finally, we test our E-invariant representations on datasets that violate Definitions 1 and 2 and the conditions of Theorem 1. We consider four vertex-attributed datasets (NCI1, NCI109, DD, PROTEINS) from Morris et al. [87], and split the data as proposed by Yehudai et al. [146]. As mentioned earlier, Yehudai et al. [146] is not part of our baselines since it requires samples from the test distribution $P(\mathcal{G}_{N^e}^{\text{te}})$.

Training and test data are created as follows: Graphs with sizes smaller than the 50-th percentile are assigned to training, while graphs with sizes larger than the 90-th percentile are assigned to test. A validation set for hyperparameter tuning consists of 10% held out examples from training.

Results. Table 3 shows the test results using the Matthews correlation coefficient (MCC) — MCC was chosen due to significant class imbalances in the OOD shift of our test data, see Appendix F for more details. We observe that always one of our E-invariant representations Γ_{GIN} and Γ_{RPGIN} is amongst the top 4 best methods in all datasets except NCI109. We also note that the WL KERNEL performs really well at NCI1 and very poorly (random) on PROTEINS and DD, showcasing the importance of consistency across datasets.

6 Conclusions

In this work we looked at the task of out-of-distribution (OOD) graph classification, where train and test data have different distributions. By introducing a structural causal model inspired by graphon models [79], we defined a representation that is approximately invariant to the train/test distribution changes of our causal model, empirically showing its benefits on both synthetic and real-world datasets against standard graph classification baselines. Finally, our work contributed a blueprint for defining graph extrapolation tasks through causal models.

Acknowledgments and Disclosure of Funding

This work was funded in part by the National Science Foundation (NSF) Awards CAREER IIS-1943364 and CCF-1918483, the Purdue Integrative Data Science Initiative, and the Wabash Heartland Innovation Network. Any opinions, findings and conclusions or recommendations expressed in this material are those of the authors and do not necessarily reflect the views of the sponsors. Further, we would like to thank Ryan Murphy for many insightful discussions, and Mayank Kakodkar and Carlos H. C. Teixeira for their invaluable help with the subgraph function estimation.

References

- [1] Ghadeer Abuoda, Gianmarco De Francisci Morales, and Ashraf Aboulnaga. Link prediction via higher-order motif features. In *Joint European Conference on Machine Learning and Knowledge Discovery in Databases*, pages 412–429. Springer, 2019.
- [2] Nesreen K Ahmed, Theodore L Willke, and Ryan A Rossi. Estimation of local subgraph counts. In *2016 IEEE International Conference on Big Data (Big Data)*, pages 586–595. IEEE, 2016.
- [3] Edo M Airoldi, Thiago B Costa, and Stanley H Chan. Stochastic blockmodel approximation of a graphon: Theory and consistent estimation. In *Advances in Neural Information Processing Systems*, pages 692–700, 2013.
- [4] David J Aldous. Representations for partially exchangeable arrays of random variables. *Journal of Multivariate Analysis*, 11(4):581–598, 1981.
- [5] Uri Alon. Network motifs: theory and experimental approaches. *Nature Reviews Genetics*, 8(6):450–461, 2007.
- [6] Anonymous. Incremental learning on growing graphs. In *Submitted to International Conference on Learning Representations*, 2021. under review.
- [7] Martin Arjovsky, Léon Bottou, Ishaan Gulrajani, and David Lopez-Paz. Invariant risk minimization. *arXiv preprint arXiv:1907.02893*, 2019.
- [8] J Scott Armstrong, Fred Collopy, and J Thomas Yokum. Decomposition by causal forces: a procedure for forecasting complex time series. *International Journal of forecasting*, 21(1):25–36, 2005.
- [9] Vikraman Arvind, Frank Fuhlbrück, Johannes Köbler, and Oleg Verbitsky. On weisfeiler-leman invariance: subgraph counts and related graph properties. *Journal of Computer and System Sciences*, 2020.
- [10] James Atwood and Don Towsley. Diffusion-convolutional neural networks. In *Advances in Neural Information Processing Systems*, pages 1993–2001, 2016.

- [11] Alexander Balke and Judea Pearl. Probabilistic evaluation of counterfactual queries. In *Proceedings of AAAI*, 1994.
- [12] Jordi Bascompte and Carlos J Melián. Simple trophic modules for complex food webs. *Ecology*, 86(11):2868–2873, 2005.
- [13] Peter Battaglia, Razvan Pascanu, Matthew Lai, Danilo Jimenez Rezende, et al. Interaction networks for learning about objects, relations and physics. In *Advances in neural information processing systems*, pages 4502–4510, 2016.
- [14] Peter W Battaglia, Jessica B Hamrick, Victor Bapst, Alvaro Sanchez-Gonzalez, Vinicius Zambaldi, Mateusz Malinowski, Andrea Tacchetti, David Raposo, Adam Santoro, Ryan Faulkner, et al. Relational inductive biases, deep learning, and graph networks. *arXiv preprint arXiv:1806.01261*, 2018.
- [15] Mikhail Belkin and Partha Niyogi. Laplacian eigenmaps and spectral techniques for embedding and clustering. In *Advances in neural information processing systems*, pages 585–591, 2002.
- [16] Irwan Bello, Hieu Pham, Quoc V Le, Mohammad Norouzi, and Samy Bengio. Neural combinatorial optimization with reinforcement learning. In *International Conference on Learning Representations*, 2017.
- [17] Yoshua Bengio, Tristan Deleu, Nasim Rahaman, Rosemary Ke, Sébastien Lachapelle, Olexa Bilaniuk, Anirudh Goyal, and Christopher Pal. A meta-transfer objective for learning to disentangle causal mechanisms. *arXiv preprint arXiv:1901.10912*, 2019.
- [18] Austin R Benson, David F Gleich, and Jure Leskovec. Higher-order organization of complex networks. *Science*, 353(6295):163–166, 2016.
- [19] Michel Besserve, Naji Shajarisales, Bernhard Schölkopf, and Dominik Janzing. Group invariance principles for causal generative models. In *International Conference on Artificial Intelligence and Statistics*, pages 557–565, 2018.
- [20] Karsten M Borgwardt and Hans-Peter Kriegel. Shortest-path kernels on graphs. In *Fifth IEEE international conference on data mining (ICDM'05)*, pages 8–pp. IEEE, 2005.
- [21] Karsten M Borgwardt, Cheng Soon Ong, Stefan Schönauer, SVN Vishwanathan, Alex J Smola, and Hans-Peter Kriegel. Protein function prediction via graph kernels. *Bioinformatics*, 21(suppl_1):i47–i56, 2005.
- [22] Giorgos Bouritsas, Fabrizio Frasca, Stefanos Zafeiriou, and Michael M Bronstein. Improving graph neural network expressivity via subgraph isomorphism counting. *arXiv preprint arXiv:2006.09252*, 2020.
- [23] Marco Bressan, Flavio Chierichetti, Ravi Kumar, Stefano Leucci, and Alessandro Panconesi. Counting graphlets: Space vs time. In *Proceedings of the Tenth ACM International Conference on Web Search and Data Mining (WSDM'17)*, pages 557–566. ACM, 2017.
- [24] Ines Chami, Zhitao Ying, Christopher Ré, and Jure Leskovec. Hyperbolic graph convolutional neural networks. In *Advances in neural information processing systems*, pages 4868–4879, 2019.
- [25] Ines Chami, Sami Abu-El-Haija, Bryan Perozzi, Christopher Ré, and Kevin Murphy. Machine learning on graphs: A model and comprehensive taxonomy. *arXiv preprint arXiv:2005.03675*, 2020.
- [26] Lina Chen, Xiaoli Qu, Mushui Cao, Yanyan Zhou, Wan Li, Binhua Liang, Weiguo Li, Weiming He, Chenchen Feng, Xu Jia, et al. Identification of breast cancer patients based on human signaling network motifs. *Scientific reports*, 3:3368, 2013.
- [27] Xiaowei Chen and John CS Lui. Mining graphlet counts in online social networks. *ACM Transactions on Knowledge Discovery from Data (TKDD)*, 12(4):1–38, 2018.
- [28] Xiaowei Chen, Yongkun Li, Pinghui Wang, and John Lui. A general framework for estimating graphlet statistics via random walk. *VLDB Endowment*, 2016.
- [29] Zhengdao Chen, Lei Chen, Soledad Villar, and Joan Bruna. Can graph neural networks count substructures? In *Advances in Neural Information Processing Systems*, 2020.
- [30] Gabriele Corso, Luca Cavalleri, Dominique Beaini, Pietro Lio, and Petar Veličković. Principal neighbourhood aggregation for graph nets. In *Advances in Neural Information Processing Systems*, 2020.
- [31] Alexander D’Amour, Katherine Heller, Dan Moldovan, Ben Adlam, Babak Alipanahi, Alex Beutel, Christina Chen, Jonathan Deaton, Jacob Eisenstein, Matthew D Hoffman, et al. Underspecification presents challenges for credibility in modern machine learning. *arXiv preprint arXiv:2011.03395*, 2020.
- [32] Manlio De Domenico, Shuntaro Sasai, and Alex Arenas. Mapping multiplex hubs in human functional brain networks. *Frontiers in neuroscience*, 10:326, 2016.

- [33] Pim de Haan, Dinesh Jayaraman, and Sergey Levine. Causal confusion in imitation learning. In *Advances in Neural Information Processing Systems*, pages 11698–11709, 2019.
- [34] Asim K Dey, Yulia R Gel, and H Vincent Poor. What network motifs tell us about resilience and reliability of complex networks. *Proceedings of the National Academy of Sciences*, 116(39):19368–19373, 2019.
- [35] Persi Diaconis and David Freedman. On the statistics of vision: the julesz conjecture. *Journal of Mathematical Psychology*, 24(2):112–138, 1981.
- [36] David K Duvenaud, Dougal Maclaurin, Jorge Iparraguirre, Rafael Bombarell, Timothy Hirzel, Alán Aspuru-Guzik, and Ryan P Adams. Convolutional networks on graphs for learning molecular fingerprints. In *Advances in neural information processing systems*, pages 2224–2232, 2015.
- [37] Dean Eckles, Brian Karrer, and Johan Ugander. Design and analysis of experiments in networks: Reducing bias from interference. *Journal of Causal Inference*, 5(1), 2016.
- [38] P Erdős and A Rényi. On random graphs i. *Publ. math. debrecen*, 6(290-297):18, 1959.
- [39] Matthias Fey and Jan E. Lenssen. Fast graph representation learning with PyTorch Geometric. In *ICLR Workshop on Representation Learning on Graphs and Manifolds*, 2019.
- [40] V. K. Garg, S. Jegelka, and T. Jaakkola. Generalization and representational limits of graph neural networks. In *Proceedings of the 37th International Conference on Machine Learning*, Proceedings of Machine Learning Research. PMLR, 2020.
- [41] Thomas Gärtner, Peter Flach, and Stefan Wrobel. On graph kernels: Hardness results and efficient alternatives. In *Learning theory and kernel machines*, pages 129–143. Springer, 2003.
- [42] Edgar N Gilbert. Random graphs. *The Annals of Mathematical Statistics*, 30(4):1141–1144, 1959.
- [43] Justin Gilmer, Samuel S. Schoenholz, Patrick F. Riley, Oriol Vinyals, and George E. Dahl. Neural message passing for quantum chemistry. In Doina Precup and Yee Whye Teh, editors, *Proceedings of the 34th International Conference on Machine Learning*, volume 70 of *Proceedings of Machine Learning Research*, pages 1263–1272, International Convention Centre, Sydney, Australia, 06–11 Aug 2017. PMLR.
- [44] Ian J. Goodfellow, Jonathon Shlens, and Christian Szegedy. Explaining and harnessing adversarial examples. In *International Conference on Learning Representations (ICLR)*, 2015.
- [45] Olivier Goudet, Diviyan Kalainathan, Philippe Caillou, Isabelle Guyon, David Lopez-Paz, and Michèle Sebag. Causal generative neural networks. *arXiv preprint arXiv:1711.08936*, 2017.
- [46] Aditya Grover and Jure Leskovec. node2vec: Scalable feature learning for networks. In *Proc. of KDD*, pages 855–864. ACM, 2016.
- [47] Patrick Haffner. Escaping the convex hull with extrapolated vector machines. In *Advances in Neural Information Processing Systems*, pages 753–760, 2002.
- [48] Aric A. Hagberg, Daniel A. Schult, and Pieter J. Swart. Exploring network structure, dynamics, and function using networkx. In Gaël Varoquaux, Travis Vaught, and Jarrod Millman, editors, *Proceedings of the 7th Python in Science Conference*, pages 11 – 15, Pasadena, CA USA, 2008.
- [49] Patric Hagmann, Maciej Kurant, Xavier Gigandet, Patrick Thiran, Van J Wedeen, Reto Meuli, and Jean-Philippe Thiran. Mapping human whole-brain structural networks with diffusion mri. *PloS one*, 2(7):e597, 2007.
- [50] Will Hamilton, Zhitao Ying, and Jure Leskovec. Inductive representation learning on large graphs. In *Advances in Neural Information Processing Systems*, pages 1024–1034, 2017.
- [51] William L. Hamilton. Graph representation learning. *Synthesis Lectures on Artificial Intelligence and Machine Learning*, 14(3):1–159, 2020.
- [52] John T Hancock and Taghi M Khoshgoftaar. Survey on categorical data for neural networks. *Journal of Big Data*, 7:1–41, 2020.
- [53] Trevor Hastie, Robert Tibshirani, and Jerome Friedman. *The elements of statistical learning*, volume 1. Springer series in statistics, 2012.
- [54] Robert L Hemminger. On reconstructing a graph. *Proceedings of the American Mathematical Society*, 20(1): 185–187, 1969.
- [55] Alex Hernández-García and Peter König. Data augmentation instead of explicit regularization. *arXiv preprint arXiv:1806.03852*, 2018.
- [56] Douglas N Hoover. Relations on probability spaces and arrays of random variables. *Technical Report, Institute for Advanced Study, Princeton, NJ*, 2, 1979.

- [57] Weihua Hu, Matthias Fey, Marinka Zitnik, Yuxiao Dong, Hongyu Ren, Bowen Liu, Michele Catasta, and Jure Leskovec. Open graph benchmark: Datasets for machine learning on graphs. In *Advances in Neural Information Processing Systems*, 2020.
- [58] Fredrik Johansson, Uri Shalit, and David Sontag. Learning representations for counterfactual inference. In *International conference on machine learning*, pages 3020–3029, 2016.
- [59] Chaitanya K Joshi, Quentin Cappart, Louis-Martin Rousseau, Thomas Laurent, and Xavier Bresson. Learning tsp requires rethinking generalization. *arXiv preprint arXiv:2006.07054*, 2020.
- [60] Olav Kallenberg. *Probabilistic symmetries and invariance principles*. Springer Science & Business Media, 2006.
- [61] Hisashi Kashima, Koji Tsuda, and Akihiro Inokuchi. Marginalized kernels between labeled graphs. In *Proceedings of the 20th international conference on machine learning (ICML-03)*, pages 321–328, 2003.
- [62] Seyed Mehran Kazemi, Rishab Goel, Kshitij Jain, Ivan Kobyzev, Akshay Sethi, Peter Forsyth, and Pascal Poupart. Representation learning for dynamic graphs: A survey. *Journal of Machine Learning Research*, 21(70):1–73, 2020.
- [63] Paul J Kelly et al. A congruence theorem for trees. *Pacific Journal of Mathematics*, 7(1):961–968, 1957.
- [64] Gary King and Langche Zeng. The dangers of extreme counterfactuals. *Political Analysis*, 14(2):131–159, 2006.
- [65] Thomas Kipf and Max Welling. Semi-supervised classification with graph convolutional networks. In *International Conference on Learning Representations*, 2017.
- [66] Thomas N Kipf and Max Welling. Variational graph auto-encoders. *NIPS Workshop on Bayesian Deep Learning*, 2016.
- [67] Johannes Klicpera, Janek Groß, and Stephan Günnemann. Directional message passing for molecular graphs. In *International Conference on Learning Representations*, 2020.
- [68] Pang Wei Koh, Shiori Sagawa, Henrik Marklund, Sang Michael Xie, Marvin Zhang, Akshay Balsubramani, Weihua Hu, Michihiro Yasunaga, Richard Lanas Phillips, Sara Beery, et al. Wilds: A benchmark of in-the-wild distribution shifts. *arXiv preprint arXiv:2012.07421*, 2020.
- [69] Nils M Kriege, Christopher Morris, Anja Rey, and Christian Sohler. A property testing framework for the theoretical expressivity of graph kernels. In *IJCAI*, pages 2348–2354, 2018.
- [70] Nils M Kriege, Fredrik D Johansson, and Christopher Morris. A survey on graph kernels. *Applied Network Science*, 5(1):1–42, 2020.
- [71] Srijan Kumar, Xikun Zhang, and Jure Leskovec. Predicting dynamic embedding trajectory in temporal interaction networks. In *Proceedings of the 25th ACM SIGKDD International Conference on Knowledge Discovery and Data Mining, KDD '19*, page 1269–1278, New York, NY, USA, 2019. Association for Computing Machinery. ISBN 9781450362016.
- [72] Guillaume Lample and François Charton. Deep learning for symbolic mathematics. In *International Conference on Learning Representations*, 2020.
- [73] John Boaz Lee, Ryan A Rossi, Xiangnan Kong, Sungchul Kim, Eunyee Koh, and Anup Rao. Higher-order graph convolutional networks. *arXiv preprint arXiv:1809.07697*, 2018.
- [74] Xing Li, Wei Wei, Xiangnan Feng, Xue Liu, and Zhiming Zheng. Representation learning of graphs using graph convolutional multilayer networks based on motifs. *arXiv preprint arXiv:2007.15838*, 2020.
- [75] Qi Liu, Maximilian Nickel, and Douwe Kiela. Hyperbolic graph neural networks. In *Advances in Neural Information Processing Systems*, pages 8230–8241, 2019.
- [76] Francesco Locatello, Stefan Bauer, Mario Lucic, Gunnar Raetsch, Sylvain Gelly, Bernhard Schölkopf, and Olivier Bachem. Challenging common assumptions in the unsupervised learning of disentangled representations. In *international conference on machine learning*, pages 4114–4124, 2019.
- [77] Christos Louizos, Uri Shalit, Joris M Mooij, David Sontag, Richard Zemel, and Max Welling. Causal effect inference with deep latent-variable models. In *Advances in Neural Information Processing Systems*, pages 6446–6456, 2017.
- [78] László Lovász. *Large networks and graph limits*, volume 60. American Mathematical Soc., 2012.
- [79] László Lovász and Balázs Szegedy. Limits of dense graph sequences. *Journal of Combinatorial Theory, Series B*, 96(6):933–957, 2006.
- [80] Shmoolik Mangan and Uri Alon. Structure and function of the feed-forward loop network motif. *Proceedings of the National Academy of Sciences*, 100(21):11980–11985, 2003.

- [81] Haggai Maron, Heli Ben-Hamu, Hadar Serviansky, and Yaron Lipman. Provably powerful graph networks. In *Advances in Neural Information Processing Systems*, pages 2156–2167, 2019.
- [82] Haggai Maron, Heli Ben-Hamu, Nadav Shamir, and Yaron Lipman. Invariant and equivariant graph networks. In *International Conference on Learning Representations*, 2019.
- [83] Brendan D McKay. Small graphs are reconstructible. *Australasian Journal of Combinatorics*, 15:123–126, 1997.
- [84] Changping Meng, S Chandra Mouli, Bruno Ribeiro, and Jennifer Neville. Subgraph pattern neural networks for high-order graph evolution prediction. In *AAAI*, pages 3778–3787, 2018.
- [85] Ron Milo, Shai Shen-Orr, Shalev Itzkovitz, Nadav Kashtan, Dmitri Chklovskii, and Uri Alon. Network motifs: simple building blocks of complex networks. *Science*, 298(5594):824–827, 2002.
- [86] Christopher Morris, Martin Ritzert, Matthias Fey, William L Hamilton, Jan Eric Lenssen, Gaurav Rattan, and Martin Grohe. Weisfeiler and leman go neural: Higher-order graph neural networks. In *Proceedings of the AAAI Conference on Artificial Intelligence*, volume 33, pages 4602–4609, 2019.
- [87] Christopher Morris, Nils M. Kriege, Franka Bause, Kristian Kersting, Petra Mutzel, and Marion Neumann. Tudataset: A collection of benchmark datasets for learning with graphs. In *ICML 2020 Workshop on Graph Representation Learning and Beyond (GRL+ 2020)*, 2020.
- [88] Elizabeth Munch. A user’s guide to topological data analysis. *Journal of Learning Analytics*, 4(2):47–61, 2017.
- [89] Ryan Murphy, Balasubramaniam Srinivasan, Vinayak Rao, and Bruno Ribeiro. Relational pooling for graph representations. In *Proceedings of the 36th International Conference on Machine Learning*, 2019.
- [90] J Neyman. Sur les applications de la theorie des probabilites aux experiences agricoles: essai des principes (masters thesis); justification of applications of the calculus of probabilities to the solutions of certain questions in agricultural experimentation. excerpts english translation (reprinted). *Stat Sci*, 5:463–472, 1923.
- [91] Mathias Niepert, Mohamed Ahmed, and Konstantin Kutzkov. Learning convolutional neural networks for graphs. In *International conference on machine learning*, pages 2014–2023, 2016.
- [92] Alex Nowak, Soledad Villar, Afonso S Bandeira, and Joan Bruna. A note on learning algorithms for quadratic assignment with graph neural networks. In *Proceeding of the 34th International Conference on Machine Learning (ICML)*, volume 1050, page 22, 2017.
- [93] Peter Orbanz and Daniel M Roy. Bayesian models of graphs, arrays and other exchangeable random structures. *IEEE transactions on pattern analysis and machine intelligence*, 37(2):437–461, 2014.
- [94] Mingdong Ou, Peng Cui, Jian Pei, Ziwei Zhang, and Wenwu Zhu. Asymmetric transitivity preserving graph embedding. In *Proceedings of the 22nd ACM SIGKDD international conference on Knowledge discovery and data mining*, pages 1105–1114, 2016.
- [95] Nicolas Papernot, Patrick McDaniel, Ian Goodfellow, Somesh Jha, Z Berkay Celik, and Ananthram Swami. Practical black-box attacks against machine learning. In *Proceedings of the 2017 ACM on Asia conference on computer and communications security*, pages 506–519, 2017.
- [96] Adam Paszke, Sam Gross, Francisco Massa, Adam Lerer, James Bradbury, Gregory Chanan, Trevor Killeen, Zeming Lin, Natalia Gimelshein, Luca Antiga, Alban Desmaison, Andreas Kopf, Edward Yang, Zachary DeVito, Martin Raison, Alykhan Tejani, Sasank Chilamkurthy, Benoit Steiner, Lu Fang, Junjie Bai, and Soumith Chintala. Pytorch: An imperative style, high-performance deep learning library. In H. Wallach, H. Larochelle, A. Beygelzimer, F. d’Alché-Buc, E. Fox, and R. Garnett, editors, *Advances in Neural Information Processing Systems 32*, pages 8024–8035. Curran Associates, Inc., 2019.
- [97] Judea Pearl. *Causality*. Cambridge university press, 2009.
- [98] F. Pedregosa, G. Varoquaux, A. Gramfort, V. Michel, B. Thirion, O. Grisel, M. Blondel, P. Prettenhofer, R. Weiss, V. Dubourg, J. Vanderplas, A. Passos, D. Cournapeau, M. Brucher, M. Perrot, and E. Duchesnay. Scikit-learn: Machine learning in Python. *Journal of Machine Learning Research*, 12:2825–2830, 2011.
- [99] Bryan Perozzi, Rami Al-Rfou, and Steven Skiena. Deepwalk: Online learning of social representations. In *Proceedings of the 20th ACM SIGKDD international conference on Knowledge discovery and data mining*, pages 701–710, 2014.
- [100] Ali Pinar, C Seshadhri, and Vaidyanathan Vishal. Escape: Efficiently counting all 5-vertex subgraphs. In *Proceedings of the 26th International Conference on World Wide Web*, pages 1431–1440, 2017.
- [101] Nataša Pržulj. Biological network comparison using graphlet degree distribution. *Bioinformatics*, 23(2):e177–e183, 2007.

- [102] Jiezhong Qiu, Yuxiao Dong, Hao Ma, Jian Li, Kuansan Wang, and Jie Tang. Network embedding as matrix factorization: Unifying deepwalk, line, pte, and node2vec. In *Proceedings of the Eleventh ACM International Conference on Web Search and Data Mining*, pages 459–467, 2018.
- [103] Anant Raj, Stefan Bauer, Ashkan Soleymani, Michel Besserve, and Bernhard Schölkopf. Causal feature selection via orthogonal search. *arXiv preprint arXiv:2007.02938*, 2020.
- [104] Bastian Rieck, Christian Bock, and Karsten Borgwardt. A persistent weisfeiler-lehman procedure for graph classification. In Kamalika Chaudhuri and Ruslan Salakhutdinov, editors, *Proceedings of the 36th International Conference on Machine Learning*, volume 97 of *Proceedings of Machine Learning Research*, pages 5448–5458, Long Beach, California, USA, 09–15 Jun 2019. PMLR.
- [105] Ryan A Rossi, Nesreen K Ahmed, and Eunyee Koh. Higher-order network representation learning. In *Companion Proceedings of the The Web Conference 2018*, pages 3–4, 2018.
- [106] Ryan A Rossi, Nesreen K Ahmed, Aldo Carranza, David Arbour, Anup Rao, Sungchul Kim, and Eunyee Koh. Heterogeneous network motifs. *arXiv preprint arXiv:1901.10026*, 2019.
- [107] Donald B Rubin. Estimating causal effects of treatments in randomized and nonrandomized studies. *Journal of educational Psychology*, 66(5):688, 1974.
- [108] Alvaro Sanchez-Gonzalez, Nicolas Heess, Jost Tobias Springenberg, Josh Merel, Martin A Riedmiller, Raia Hadsell, and Peter Battaglia. Graph networks as learnable physics engines for inference and control. In *International Conference on Machine Learning*, 2018.
- [109] Adam Santoro, Felix Hill, David Barrett, Ari Morcos, and Timothy Lillicrap. Measuring abstract reasoning in neural networks. In *International Conference on Machine Learning*, pages 4477–4486, 2018.
- [110] Ryoma Sato. A survey on the expressive power of graph neural networks. *arXiv preprint arXiv:2003.04078*, 2020.
- [111] David Saxton, Edward Grefenstette, Felix Hill, and Pushmeet Kohli. Analysing mathematical reasoning abilities of neural models. In *International Conference on Learning Representations*, 2019.
- [112] Bernhard Schölkopf. Causality for machine learning. *arXiv preprint arXiv:1911.10500*, 2019.
- [113] J Scott Armstrong and Fred Collopy. Causal forces: Structuring knowledge for time-series extrapolation. *Journal of Forecasting*, 12(2):103–115, 1993.
- [114] Naji Shajarisales, Dominik Janzing, Bernhard Schoelkopf, and Michel Besserve. Telling cause from effect in deterministic linear dynamical systems. In *International Conference on Machine Learning*, pages 285–294. PMLR, 2015.
- [115] Shai S Shen-Orr, Ron Milo, Shmoolik Mangan, and Uri Alon. Network motifs in the transcriptional regulation network of *escherichia coli*. *Nature genetics*, 31(1):64–68, 2002.
- [116] Nino Shervashidze, SVN Vishwanathan, Tobias Petri, Kurt Mehlhorn, and Karsten Borgwardt. Efficient graphlet kernels for large graph comparison. In *Artificial Intelligence and Statistics*, pages 488–495, 2009.
- [117] Nino Shervashidze, Pascal Schweitzer, Erik Jan van Leeuwen, Kurt Mehlhorn, and Karsten M Borgwardt. Weisfeiler-lehman graph kernels. *Journal of Machine Learning Research*, 12(Sep):2539–2561, 2011.
- [118] Chawin Sitawarin, Arjun Nitin Bhagoji, Arsalan Mosenia, Prateek Mittal, and Mung Chiang. Rogue signs: Deceiving traffic sign recognition with malicious ads and logos. *CoRR*, abs/1801.02780, 2018.
- [119] Tom AB Snijders and Krzysztof Nowicki. Estimation and prediction for stochastic blockmodels for graphs with latent block structure. *Journal of classification*, 14(1):75–100, 1997.
- [120] Olaf Sporns and Rolf Kötter. Motifs in brain networks. *PLoS biology*, 2(11):e369, 2004.
- [121] Lewi Stone and Alan Roberts. Competitive exclusion, or species aggregation? *Oecologia*, 91(3):419–424, 1992.
- [122] Lewi Stone, Daniel Simberloff, and Yael Artzy-Randrup. Network motifs and their origins. *PLoS computational biology*, 15(4):e1006749, 2019.
- [123] Mahito Sugiyama, M. Elisabetta Ghisu, Felipe Llinares-López, and Karsten Borgwardt. graphkernels: R and python packages for graph comparison. *Bioinformatics*, 34(3):530–532, 2017.
- [124] Masashi Sugiyama, Matthias Krauledat, and Klaus-Robert Müller. Covariate shift adaptation by importance weighted cross validation. *Journal of Machine Learning Research*, 8(5), 2007.
- [125] Haitian Sun, Bhuwan Dhingra, Manzil Zaheer, Kathryn Mazaitis, Ruslan Salakhutdinov, and William Cohen. Open domain question answering using early fusion of knowledge bases and text. In *Proceedings of the 2018 Conference on Empirical Methods in Natural Language Processing*, pages 4231–4242, Brussels, Belgium, October–November 2018. Association for Computational Linguistics.

- [126] Carlos HC Teixeira, Leornaldo Cotta, Bruno Ribeiro, and Wagner Meira. Graph pattern mining and learning through user-defined relations. In *2018 IEEE International Conference on Data Mining (ICDM)*, pages 1266–1271. IEEE, 2018.
- [127] Komal K. Teru, Etienne Denis, and William L. Hamilton. Inductive relation prediction by subgraph reasoning. In *Proceedings of the 37th International Conference on Machine Learning*, Proceedings of Machine Learning Research. PMLR, 2020.
- [128] Jin Tian and Judea Pearl. Causal discovery from changes. *UAI*, 2001.
- [129] Jan Toenshoff, Martin Ritzert, Hinrikus Wolf, and Martin Grohe. Graph learning with 1d convolutions on random walks. *arXiv preprint arXiv:2102.08786*, 2021.
- [130] Maurice CK Tweedie. Inverse statistical variates. *Nature*, 155(3937):453–453, 1945.
- [131] Stanislaw M Ulam. A collection of mathematical problems. *Wiley, New York*, 29, 1960.
- [132] Petar Veličković, Guillem Cucurull, Arantxa Casanova, Adriana Romero, Pietro Lio, and Yoshua Bengio. Graph attention networks. *ICLR*, 2018.
- [133] Petar Veličković, Rex Ying, Matilde Padovano, Raia Hadsell, and Charles Blundell. Neural execution of graph algorithms. In *International Conference on Learning Representations (ICLR)*, 2020.
- [134] Clement Vignac, Andreas Loukas, and Pascal Frossard. Building powerful and equivariant graph neural networks with structural message-passing. In *Advances in Neural Information Processing Systems*, 2020.
- [135] Nikil Wale, Ian A Watson, and George Karypis. Comparison of descriptor spaces for chemical compound retrieval and classification. *Knowledge and Information Systems*, 14(3):347–375, 2008.
- [136] Li Wang, Hongying Zhao, Jing Li, Yingqi Xu, Yujia Lan, Wenkang Yin, Xiaoqin Liu, Lei Yu, Shihua Lin, Michael Yifei Du, et al. Identifying functions and prognostic biomarkers of network motifs marked by diverse chromatin states in human cell lines. *Oncogene*, 39(3):677–689, 2020.
- [137] Pinghui Wang, John CS Lui, Bruno Ribeiro, Don Towsley, Junzhou Zhao, and Xiaohong Guan. Efficiently estimating motif statistics of large networks. *ACM Transactions on Knowledge Discovery from Data (TKDD)*, 9(2):1–27, 2014.
- [138] Yiwei Wang, Wei Wang, Yuxuan Liang, Yujun Cai, and Bryan Hooi. Graphcrop: Subgraph cropping for graph classification. *arXiv preprint arXiv:2009.10564*, 2020.
- [139] Van J Wedeen, Patric Hagmann, Wen-Yih Isaac Tseng, Timothy G Reese, and Robert M Weisskoff. Mapping complex tissue architecture with diffusion spectrum magnetic resonance imaging. *Magnetic resonance in medicine*, 54(6):1377–1386, 2005.
- [140] Zonghan Wu, Shirui Pan, Fengwen Chen, Guodong Long, Chengqi Zhang, and S Yu Philip. A comprehensive survey on graph neural networks. *IEEE Transactions on Neural Networks and Learning Systems*, 2020.
- [141] Keyulu Xu, Chengtao Li, Yonglong Tian, Tomohiro Sonobe, Ken-ichi Kawarabayashi, and Stefanie Jegelka. Representation learning on graphs with jumping knowledge networks. In *International Conference on Machine Learning*, pages 5453–5462. PMLR, 2018.
- [142] Keyulu Xu, Weihua Hu, Jure Leskovec, and Stefanie Jegelka. How powerful are graph neural networks? In *International Conference on Learning Representations*, 2019.
- [143] Keyulu Xu, Mozhi Zhang, Jingling Li, Simon Shaolei Du, Ken-Ichi Kawarabayashi, and Stefanie Jegelka. How neural networks extrapolate: From feedforward to graph neural networks. In *International Conference on Learning Representations*, 2021.
- [144] Pinar Yanardag and SVN Vishwanathan. Deep graph kernels. In *Proceedings of the 21th ACM SIGKDD International Conference on Knowledge Discovery and Data Mining*, pages 1365–1374. ACM, 2015.
- [145] Wei Ye, Omid Askarischani, Alex Jones, and Ambuj Singh. Deepmap: Learning deep representations for graph classification. *arXiv preprint arXiv:2004.02131*, 2020.
- [146] Gilad Yehudai, Ethan Fetaya, Eli Meirom, Gal Chechik, and Haggai Maron. On size generalization in graph neural networks. *arXiv preprint arXiv:2010.08853*, 2020.
- [147] Jiaxuan You, Rex Ying, and Jure Leskovec. Position-aware graph neural networks. In *International Conference on Machine Learning*, pages 7134–7143. PMLR, 2019.
- [148] Wenchao Yu, Cheng Zheng, Wei Cheng, Charu C Aggarwal, Dongjin Song, Bo Zong, Haifeng Chen, and Wei Wang. Learning deep network representations with adversarially regularized autoencoders. In *Proc. of AAAI*, pages 2663–2671. ACM, 2018.

- [149] Muhan Zhang and Yixin Chen. Link prediction based on graph neural networks. In *Advances in Neural Information Processing Systems*, pages 5165–5175, 2018.
- [150] Ziwei Zhang, Peng Cui, and Wenwu Zhu. Deep learning on graphs: A survey. *IEEE Transactions on Knowledge and Data Engineering*, 2020.

A Proof of Proposition 1

Proposition 1. [E-invariant Representation's Effect on Classification] Consider a permutation-invariant graph representation $\Gamma : \cup_{n=1}^{\infty} \{0, 1\}^{n \times n} \times \mathbb{X}^n \rightarrow \mathbb{R}^d$, $d \geq 1$, and a downstream function $\rho : \mathbb{Y} \times \mathbb{R}^d \rightarrow [0, 1]$ (e.g., a feedforward neural network (MLP) with softmax outputs) such that, for some $\epsilon, \delta > 0$, the generalization error over the training distribution is: For $\forall y \in \mathbb{Y}$,

$$P(|P(Y = y | \mathcal{G}_{N^{tr}}^{tr}) - \rho(y, \Gamma(\mathcal{G}_{N^{tr}}^{tr}))| \leq \epsilon) \geq 1 - \delta,$$

Γ is said to be **environment-invariant (E-invariant)** if $\forall e \in \text{supp}(E^{tr}), \forall e^{\dagger} \in \text{supp}(E^{te})$,

$$\Gamma(\mathcal{G}_{N^{tr}}^{tr} | E^{tr} = e) = \Gamma(\mathcal{G}_{N^{te}}^{te} | E^{te} = e^{\dagger}).$$

Then, the OOD test error is the same as the generalization error over the training distribution, i.e., for $\forall y \in \mathbb{Y}$,

$$P(|P(Y = y | \mathcal{G}_{N^{te}}^{te}) - \rho(y, \Gamma(\mathcal{G}_{N^{te}}^{te}))| \leq \epsilon) \geq 1 - \delta. \quad (3)$$

Proof. First note that Y is only a function of W and an independent random noise (following Definitions 1 and 2, depicted in Figure 1). Therefore, Y is E-invariant, and thus

$$\begin{aligned} P(Y | \mathcal{G}_{N^{te}}^{te} = G_{N^{te}}^{te}) &= \sum_{e^{\dagger} \in \text{supp}(E^{te})} P(Y | \mathcal{G}_{N^{te}}^{te} = G_{N^{te}}^{te}, E^{te} = e^{\dagger}) P(E^{te} = e^{\dagger}) \\ &= \sum_{e \in \text{supp}(E^{tr})} P(Y | \mathcal{G}_{N^{tr}}^{tr} = G_{N^{tr}}^{tr}, E^{tr} = e) P(E^{tr} = e) \\ &= P(Y | \mathcal{G}_{N^{tr}}^{tr} = G_{N^{tr}}^{tr}). \end{aligned}$$

Note above that the observed graphs in test ($G_{N^{te}}^{te}$) and train ($G_{N^{tr}}^{tr}$) change due to the change in environments. The definition of E-invariance states that $\forall e \in \text{supp}(E^{tr}), \forall e^{\dagger} \in \text{supp}(E^{te})$,

$$\Gamma(\mathcal{G}_{N^{tr}}^{tr} | E^{tr} = e) = \Gamma(\mathcal{G}_{N^{te}}^{te} | E^{te} = e^{\dagger}).$$

Finally, the E-invariance of Γ yields $\rho(y, \Gamma(\mathcal{G}_{N^{tr}}^{tr})) = \rho(y, \Gamma(\mathcal{G}_{N^{te}}^{te}))$, concluding our proof.

PS: Note that using the above equalities, Equation (2) can be adapted to yield for any graph G :

$$\begin{aligned} P(Y | \Gamma(\mathcal{G}_{N^{te}}^{te}) = \Gamma(G)) \\ = \sum_{e^{\dagger} \in \text{supp}(E^{tr})} P(Y | \Gamma(\mathcal{G}_{N^{tr}}^{tr}) = \Gamma(G), E^{tr} = e^{\dagger}) P(E^{tr} = e^{\dagger}). \end{aligned}$$

□

B Proof of Theorem 1

Theorem 1 (Approximate E-invariant Graph Representation). *Let $\mathcal{G}_{N^{tr}}^{tr}$ and $\mathcal{G}_{N^{te}}^{te}$ be two samples of graphs of sizes N^{tr} and N^{te} from the training and test distributions, respectively, both defined over the same graphon variable W and satisfying Definitions 1 and 2. Assume the vertex attribute function $g_X(\cdot)$ of Definitions 1 and 2 is invariant to E^{tr} and E^{te} (the reason for this assumption will be clear later). Let $\|\cdot\|_{\infty}$ denotes the L-infinity norm. For any integer $k \leq \min(N^{tr}, N^{te})$, and any constant $0 < \epsilon < 1$,*

$$P(\|\Gamma_{1\text{-hot}}(\mathcal{G}_{N^{tr}}^{tr}) - \Gamma_{1\text{-hot}}(\mathcal{G}_{N^{te}}^{te})\|_{\infty} > \epsilon) \leq 2|\mathcal{F}_{\leq k}|(\exp(-\frac{\epsilon^2 N^{tr}}{8k^2}) + \exp(-\frac{\epsilon^2 N^{te}}{8k^2})). \quad (10)$$

Proof. We first replace t_{ind} by t_{inj} , which is defined by

$$t_{\text{inj}}(F_k, \mathcal{G}_{N^*}^*) = \frac{\text{inj}(F_k, \mathcal{G}_{N^*}^*)}{N^*!/(N^* - k)!}, \quad (11)$$

where $\text{inj}(F_k, \mathcal{G}_{N^*}^*)$ is the number of injective homomorphisms of F_k into $\mathcal{G}_{N^*}^*$. We will justify this replacement later. Then, we know from Lovász and Szegedy [79, Theorem 2.5] that for unattributed graphs $\mathcal{G}_{N^*}^*$,

$$P(|t_{\text{inj}}(F_k, \mathcal{G}_{N^*}^*) - t(F_k, W)| > \epsilon) \leq 2 \exp(-\frac{\epsilon^2}{2k^2} N^*). \quad (12)$$

Here W is the graphon function as illustrated in Definitions 1 and 2. As defined in Lovász and Szegedy [79],

$$t(F_k, W) = \int_{[0,1]^k} \prod_{ij \in E(F_k)} W(x_i, x_j) dx_1 \cdots dx_k,$$

where $E(F_k)$ denotes the edge set of F_k . This bound shows that $t_{\text{inj}}(F_k, \mathcal{G}_{N^*}^*)$ converges to $t(F_k, W)$ as $N^* \rightarrow \infty$. Actually, we can get similar bounds for t_{ind} using the similar proof technique. Although the value it converges to is different, the difference between values is preserved as will be proved in the following text. More importantly, it can be extended to vertex-attributed graphs under our SCM assumptions depicted in Definitions 1 and 2.

We can do this because for vertex-attributed graphs, in Definitions 1 and 2, g_X operates on attributed graphs similarly as the graphon on unattributed graphs. We can consider the graph generation procedure as first generate the underlying structure, and then add vertex attribute accordingly to its corresponding random graphon value $U_v \in \text{Uniform}(0, 1)$ and graphon W . $g_X(\cdot, \cdot)$ being invariant to E^{tr} and E^{te} means for any two environment $e \in \text{supp}(E^{\text{tr}}), e^\dagger \in \text{supp}(E^{\text{te}})$, $g_X(e, \cdot) = g_X(e^\dagger, \cdot)$.

Then for a given k -vertices vertex-attributed graph F_k and a given N^* , we can define ϕ as an induced map $\phi : [k] \rightarrow [N^*]$, which can be thought about as how the k vertices in F_k are mapped to the vertices in $\mathcal{G}_{N^*}^*$. A_ϕ denotes the event ϕ is a homomorphism from F_k to the W -random graph $\mathcal{G}_{N^*}^*$. We define \mathcal{G}_m^* as the subgraph of $\mathcal{G}_{N^*}^*$ induced by vertices $\{1, \dots, m\}$. Note here m has two meanings. First, it represents the m -th vertex. Second, it also indicates the size of the subgraph. We define $B_m = \frac{1}{\binom{N^*}{k}} \sum_\phi P(A_\phi | \mathcal{G}_m^*)$, $0 \leq m \leq N^*$ as the expected induced homomorphism densities once we observe the subgraph \mathcal{G}_m^* . Here $B_0 = \frac{1}{\binom{N^*}{k}} \sum_\phi P(A_\phi)$ denotes the expectation before we observe any vertices.

B_m is a martingale for unattributed graphs (Theorem 2.5 of [79]). And since in Definitions 1 and 2 we also use the graphon W and the g_X operates on attributed graphs using the graphon W and U_v , it is also a martingale here. We do not need to care about the environment variable E^* here because the function g_X is invariant of E^* and, therefore, it can be treated as a constant. Then,

$$\begin{aligned} |B_m - B_{m-1}| &= \frac{1}{\binom{N^*}{k}} \left| \sum_\phi P(A_\phi | \mathcal{G}_m^*) - P(A_\phi | \mathcal{G}_{m-1}^*) \right| \\ &\leq \frac{1}{\binom{N^*}{k}} \sum_\phi |P(A_\phi | \mathcal{G}_m^*) - P(A_\phi | \mathcal{G}_{m-1}^*)|. \end{aligned}$$

Here, for all $\phi : [k] \rightarrow [N^*]$ that does not contain the value m in its image (which means no vertex in F_k is mapped to the m -th vertex in $\mathcal{G}_{N^*}^*$), the difference is 0. For all other terms, the terms are at most 1. Thus,

$$|B_m - B_{m-1}| \leq \frac{\binom{N^*-1}{k-1}}{\binom{N^*}{k}} = \frac{k}{n}.$$

By definition, $B_0 = \frac{1}{\binom{N^*}{k}} \sum_\phi P(A_\phi) = t^*(F_k, W)$, and $B_{N^*} = \frac{1}{\binom{N^*}{k}} \text{ind}(F_k, \mathcal{G}_{N^*}^*) = t_{\text{ind}}(F_k, \mathcal{G}_{N^*}^*)$, where $t^*(F_k, W)$ is defined as B_0 – the expected induced homomorphism densities if we only know the graphon W and did not observe any vertex in the graph.

Then, we can use Azuma's inequality for Martingales,

$$\begin{aligned} P(B_{N^*} - B_0 > \epsilon) &\leq \exp\left(-\frac{\epsilon^2}{2N^*(k/N^*)^2}\right) \\ &= \exp\left(-\frac{\epsilon^2}{2k^2} N^*\right). \end{aligned}$$

Since $B_{N^*} = t_{\text{ind}}(F_k, \mathcal{G}_{N^*}^*)$, and $B_0 = t^*(F_k, W)$, we get the similar bound as in Equation (12),

$$P(|t_{\text{ind}}(F_k, \mathcal{G}_{N^*}^*) - t^*(F_k, W)| > \epsilon) \leq 2 \exp\left(-\frac{\epsilon^2}{2k^2} N^*\right).$$

Since $|t_{\text{ind}}(F_k, \mathcal{G}_{N^{\text{tr}}}^{\text{tr}}) - t^*(F_k, W)| \leq \frac{\epsilon}{2}$, $|t_{\text{ind}}(F_k, \mathcal{G}_{N^{\text{te}}}^{\text{te}}) - t^*(F_k, W)| \leq \frac{\epsilon}{2}$ implies $|t_{\text{ind}}(F_k, \mathcal{G}_{N^{\text{tr}}}^{\text{tr}}) - t_{\text{ind}}(F_k, \mathcal{G}_{N^{\text{te}}}^{\text{te}})| \leq \epsilon$, we have,

$$\begin{aligned}
& \mathbb{P}(|t_{\text{ind}}(F_k, \mathcal{G}_{N^{\text{tr}}}^{\text{tr}}) - t_{\text{ind}}(F_k, \mathcal{G}_{N^{\text{te}}}^{\text{te}})| > \epsilon) \\
&= 1 - \mathbb{P}(|t_{\text{ind}}(F_k, \mathcal{G}_{N^{\text{tr}}}^{\text{tr}}) - t_{\text{ind}}(F_k, \mathcal{G}_{N^{\text{te}}}^{\text{te}})| \leq \epsilon) \\
&\leq 1 - \mathbb{P}(|t_{\text{ind}}(F_k, \mathcal{G}_{N^{\text{tr}}}^{\text{tr}}) - t^*(F_k, W)| \leq \frac{\epsilon}{2}) \\
&\quad \cdot \mathbb{P}(|t_{\text{ind}}(F_k, \mathcal{G}_{N^{\text{te}}}^{\text{te}}) - t^*(F_k, W)| \leq \frac{\epsilon}{2}) \\
&\leq 1 - (1 - 2 \exp(-\frac{\epsilon^2}{8k^2} N^{\text{tr}}))(1 - 2 \exp(-\frac{\epsilon^2}{8k^2} N^{\text{te}})) \\
&= 2(\exp(-\frac{\epsilon^2}{8k^2} N^{\text{tr}}) + \exp(-\frac{\epsilon^2}{8k^2} N^{\text{te}})) \\
&\quad - 4 \exp(-\frac{\epsilon^2}{8k^2} (N^{\text{tr}} + N^{\text{te}})) \\
&\leq 2(\exp(-\frac{\epsilon^2}{8k^2} N^{\text{tr}}) + \exp(-\frac{\epsilon^2}{8k^2} N^{\text{te}})).
\end{aligned} \tag{13}$$

Then we know,

$$\begin{aligned}
& \mathbb{P}(\|\Gamma_{1\text{-hot}}(\mathcal{G}_{N^{\text{tr}}}^{\text{tr}}) - \Gamma_{1\text{-hot}}(\mathcal{G}_{N^{\text{te}}}^{\text{te}})\|_{\infty} \leq \epsilon) \\
&= \mathbb{P}(|t_{\text{ind}}(F_{k'}, \mathcal{G}_{N^{\text{tr}}}^{\text{tr}}) - t_{\text{ind}}(F_{k'}, \mathcal{G}_{N^{\text{te}}}^{\text{te}})| \leq \epsilon, \forall F_{k'} \in \mathcal{F}_{\leq k}) \\
&\geq 1 - \sum_{F_{k'} \in \mathcal{F}_{\leq k}} \mathbb{P}(|t_{\text{ind}}(F_{k'}, \mathcal{G}_{N^{\text{tr}}}^{\text{tr}}) - t_{\text{ind}}(F_{k'}, \mathcal{G}_{N^{\text{te}}}^{\text{te}})| > \epsilon) \\
&\geq 1 - 2|\mathcal{F}_{\leq k}|(\exp(-\frac{\epsilon^2 N^{\text{tr}}}{8k^2}) + \exp(-\frac{\epsilon^2 N^{\text{te}}}{8k^2})).
\end{aligned} \tag{14}$$

It follows from the Bonferroni inequality that $\mathbb{P}(\cap_{i=1}^N A_i) \geq 1 - \sum_{i=1}^N \mathbb{P}(\tilde{A}_i)$, where A_i and its complement \tilde{A}_i are any events. Therefore,

$$\mathbb{P}(\|\Gamma_{1\text{-hot}}(\mathcal{G}_{N^{\text{tr}}}^{\text{tr}}) - \Gamma_{1\text{-hot}}(\mathcal{G}_{N^{\text{te}}}^{\text{te}})\|_{\infty} > \epsilon) \leq 2|\mathcal{F}_{\leq k}|(\exp(-\frac{\epsilon^2 N^{\text{tr}}}{8k^2}) + \exp(-\frac{\epsilon^2 N^{\text{te}}}{8k^2})),$$

concluding the proof. \square

C Biases in estimating induced homomorphism densities

Induced (connected) homomorphism densities of a given graph $F_{k'}$ over all possible k' -vertex ($k' \leq k$) connected graph for an N^* -vertex graph $\mathcal{G}_{N^*}^*$ are defined as

$$\omega(F_{k'}, \mathcal{G}_{N^*}^*) = \frac{\text{ind}(F_{k'}, \mathcal{G}_{N^*}^*)}{\sum_{F_{k'} \in \mathcal{F}_{\leq k}} \text{ind}(F_{k'}, \mathcal{G}_{N^*}^*)}.$$

This is a slightly different definition from the induced homomorphism densities in Equation (4). In the main text, the denominator is the total number of possible mappings (which can include mappings that are disconnected). Here we mainly consider the total numbers of induced mappings that are connected.

Achieving unbiased estimates for induced (connected) homomorphism densities usually requires sophisticated methods and enormous amount of time. We show that a biased estimator can also work for the GNN^+ in Equation (8) if the bias is multiplicative and the READOUT_{Γ} is simply the sum of the vertex embeddings. We formalize it as followed.

Proposition 2. *Assume $\hat{\omega}(F_{k'}, \mathcal{G}_{N^*}^*)$ is a biased estimator for $\omega(F_{k'}, \mathcal{G}_{N^*}^*)$ for any k' and k' -sized connected graphs $F_{k'}$ in a N^* -vertex $\mathcal{G}_{N^*}^*$, such that $\mathbb{E}(\hat{\omega}(F_{k'}, \mathcal{G}_{N^*}^*)) = \beta(F_{k'})\omega(F_{k'}, \mathcal{G}_{N^*}^*)$, where $\beta(F_{k'})$ ($\beta(\cdot) > 0$) is the bias related to the graph $F_{k'}$, and the expectation is over the sampling procedure. The expected learned representation $\mathbb{E}(\sum_{F_{k'} \in \mathcal{F}_{\leq k}} \hat{\omega}(F_{k'}, \mathcal{G}_{N^*}^*) \mathbf{1}^T (\text{GNN}^+(F_{k'})))$ can be the same as using the true induced (connected) homomorphism densities $\omega(F_{k'}, \mathcal{G}_{N^*}^*)$, $\forall F_{k'} \in \mathcal{F}_{\leq k}$.*

Proof. W.L.O.G, assume $\text{GNN}_0^+(F_{k'})$ is the representation we can learn from the true induced (connected) homomorphism densities $\omega(F_{k'}, \mathcal{G}_{N^*}^*)$, $\forall F_{k'} \in \mathcal{F}_{\leq k}$. When only using the biased estimators, if we are able to learn the

representation $\text{GNN}^+(F_{k'}) = \text{GNN}_0^+(F_{k'})/\beta(F_{k'})$ for all $F_{k'} \in \mathcal{F}_{\leq k}$, then we can still get the graph representation in Equation (8) the same as using the true induced (connected) homomorphism densities. This is possible because GNN^+ is proven to be a most expressive k' -vertex graph representation, thus it is able to learn any function on the graph $F_{k'}$. Then,

$$\mathbb{E} \left[\sum_{F_{k'} \in \mathcal{F}_{\leq k}} \hat{\omega}(F_{k'}, \mathcal{G}_{N^*}^*) \mathbf{1}^T(\text{GNN}^+(F_{k'})) \right] = \sum_{F_{k'} \in \mathcal{F}_{\leq k}} \omega(F_{k'}, \mathcal{G}_{N^*}^*) \mathbf{1}^T(\text{GNN}_0^+(F_{k'})), \quad (15)$$

where $\mathbf{1}^T(\text{GNN}^+(F_{k'}))$ is the sum of the vertex embeddings given by the GNN^+ if it is an equivariant representation of the graph. \square

D Review of Graph Neural Networks

Graph Neural Networks (GNNs) constitute a popular class of methods for learning representations of vertices in a graph or graph-wide representations [65, 10, 50, 43, 132, 142, 86, 147, 75, 24]. We will explain the general case of learning graph-wide representations but the idea applies straightforwardly to applying GNNs to connected induced subgraphs in a larger graph to learn their latent representations. That is, in our work, we have applied GNNs to connected induced subgraphs in a graph, and then aggregated them to obtain the representation of the graph. We briefly summarize the idea, but more details can be found in texts such as by Hamilton [51] and reviews by Wu et al. [140] and Zhang et al. [150] and the references therein.

Suppose we have a graph G with vertex set $V = \{1, 2, \dots, N\}$, and each vertex in our data may carry some vertex feature (also called an *attribute*). For instance, in a molecule, vertices may represent atoms, edges may represent bonds, and features may indicate the atomic number [36]. These vertex features can be stored in an $N \times d$ matrix \mathbf{X} , where d is the dimension of the vertex feature vector. In particular, row $v \in V$ of X_v holds the attribute associated with vertex v .

Simply speaking, GNNs proceed by vertices passing messages, amongst each other, passing these through a learnable function such as an MLP, and repeating $T \in \mathbb{Z}_{\geq 1}$ times. At each iteration $t = \{1, 2, \dots, T\}$, all vertices $v \in V$ are associated with a learned vector $\mathbf{h}_v^{(t)}$. Specifically, we begin by initializing a vector as $\mathbf{h}_v^{(0)} = X_v$ for every vertex $v \in V$. Then, we recursively compute an update such as the following

$$\mathbf{h}_v^{(t)} = \text{MLP}^{(t)} \left(\mathbf{h}_v^{(t-1)}, \sum_{u \in \mathcal{N}(v)} \mathbf{h}_u^{(t-1)} \right), \quad \forall v \in V, \quad (16)$$

where $\mathcal{N}(v) \subseteq V$ denotes the neighborhood set of v in the graph, $\text{MLP}^{(t)}$ denotes a multi-layer perceptron, and whose superscript t indicates that the MLP at each recursion layer may have different learnable parameters. We can replace the summation with any permutation-invariant function of the neighborhood. We see that GNNs recursively update vertex states with states from their neighbors and their state from the previous recursion layer. Additionally, we can sample from the neighborhood set rather than aggregating over every neighbor. Generally speaking there is much research into the variations of this recursion step and we refer the reader to aforementioned references for details.

To learn a graph representation, we can aggregate the vertex representations using a so-called *READOUT* function defined to be permutation-invariant over the labels. A graph representation \mathbf{h}_G by a GNN is thus

$$\mathbf{h}_G = \text{READOUT} \left(\{\mathbf{h}_v^{(t)}\}_{v \in V \times \{1, \dots, T\}} \right)$$

where the vertex features $\mathbf{h}_v^{(t)}$ are as in Equation (16). READOUT may or may not contain learnable weights. We denote it as *XU-READOUT* to not confuse with our notation READOUT_{Γ} .

The entire function is differentiable and can be learned end-to-end. These models are thus typically trained with variants of Stochastic Gradient Descent. In our work, we apply this scheme over connected induced subgraphs in the graph, making them a differentiable module in our end-to-end representation scheme.

E Further Related Work

This section provides a more in-depth discussion placing our work in the context of existing literature. We explain why existing state-of-the-art graph learning methods will struggle to extrapolate, subgraph methods, and explore perspectives of causality and extrapolation at large as well as in the context of graph classification.

Causal reasoning and invariances. Recent efforts have brought counterfactual inference to machine learning models, including *Independence of causal mechanism (ICM)* methods [17, 19, 58, 77, 103, 112], *Causal Discovery from Change (CDC)* methods [128], and *representation disentanglement* methods [17, 45, 76]. Invariant risk minimization (IRM) [7] is a type of ICM [112]. Broadly, these efforts look for representations (or mechanism descriptions) that are invariant across multiple environments observed in the training data. In our work, we are interested in techniques that can work with a single training environment and when the test support is not a subset of the train support—a common case in graph data. Moreover, these works are not specifically designed for graphs, and it is unclear how they can be efficiently adapted for graph tasks. To the best of our knowledge there is no clear effort for counterfactual graph extrapolations from a single environment.

Extrapolation. Geometrically, extrapolation can be thought as reasoning beyond a convex hull of a set of training points [53, 47, 64, 143]. However, for neural networks—and their arbitrary representation mappings—this geometric interpretation is insufficient to describe a truly broad range of tasks. Rather, extrapolations are better described through counterfactual reasoning [90, 107, 97, 112].

There are other approaches for conferring models with extrapolation abilities. These ideas have started to permeate graph literature, which we touch on here, but remain outside the scope of our systematic counterfactual modeling framework.

Incorporating domain knowledge is an intuitive approach to learn a function that predicts adequately outside of the training distribution, data collection environment, and heuristic curation. This has been used, for example, in time series forecasting [113, 8]. This can come in the form of re-expressing phenomena in a way that can be adequately and accurately represented by machine learning methods [72] or specifically augmenting existing general-purpose methods to task [67]. In the context of graphs, it has been used to pre-process the graph input to make a learned graph neural network model a less complex function and thus extend beyond training data [143], although this does not necessarily fall into the framework we consider here.

Another way of moving beyond the training data is *robustness*. Relevant for deep learning systems are adversarial attacks [95]. Neural networks can be highly successful classifiers on the training data but become wildly inaccurate with small perturbations of those training examples [44]. This is important, say, in self-driving cars [118], which can become confused by graffiti. This becomes particularly problematic when we deploy systems to real-world environments outside the training data. Learning to defend against adversarial attacks is in a way related to performing well outside the environment and curation heuristics encountered in training. An interesting possibility for future work is to explore the relationships between the two approaches.

Overfitting will compromise even generalization (interpolation). Regularization schemes such as explicit penalization are a well known and broadly applicable strategy [53]. Another implicit approach is data augmentation [55], and the recent GraphCrop method proposes a scheme for graphs that randomly extracts subgraphs from certain graphs in a minibatch during training [138]. These directions differ from our own in that we seek a formulation for extrapolation even when overfitting is not necessarily a problem but the two approaches are both useful in the toolbox of an analyst.

We would like to point out that representation learning on *dynamic graphs* [62], including tasks like link prediction on growing graphs [6], is a separate vein of work from what we consider here. In these scenarios, there is a direct expectation that the process we model will change and evolve. For instance, knowledge bases – a form of graph encoding facts and relationships – are inevitably incomplete [125]. Simply put, developments in information and society move faster than they can be curated. Another important example is recommendation systems [71] based on evolving user-item networks. These concepts are related to the counterfactuals on graphs [37] that we discuss. This is fundamentally different from our work where we do graph-wide learning and representation of a dataset of many graphs rather than one constantly evolving graph.

Subgraph methods and Graphlet Counting Kernels. A foundational principle here is that exploiting subgraphs confers graph classifications models with both the ability to fit the training data and extrapolate to graphs generated from a different environment. As detailed in Section 3.2, this insight follows from the Aldous-Hoover representation exchangeable distributions over graphs [56, 4, 60, 93] and work on graph limits [78]. We discuss the large literature using subgraphs in machine learning.

Counting kernels [116] measure the similarity between two graphs by the dot product of their normalized counts of connected induced subgraphs (graphlet). This can be used for classification via kernelized methods like Support Vector Machines (SVM). Yanardag and Vishwanathan [144] argue that the dot product does not capture dependence between subgraphs and extend to a general bilinear form over a learned similarity matrix. These approaches are related to the Reconstruction Conjecture, which posits graphs can be determined through knowledge of their subgraphs [63, 131, 54, 83]. It is known that computing a maximally expressive graph kernel, or one that is injective over the class of graphs, is

as hard as the Graph Isomorphism problem, and thus intractable in general [41, 70]. Kriege et al. [69] demonstrate graph properties that subgraph counting kernels fail to capture and propose a method to make them more expressive, but only for graphs without vertex attributes. Most applications of graphlet counting do not exploit vertex attributes, and even those that do (e.g. [135]) are likely to fail under a distribution shift over attributes; recording a count for each type of attributed subgraph (e.g. red clique, blue clique) is sensitive to distribution shift. In comparison, our use of Relational Pooling Graph Neural Networks confers our framework with the ability learn a compressed representation of different attributed subgraphs, tailored for the task, and extrapolate even under attribute shift. We demonstrate this in the experiments below. Last, a recent work of Ye et al. [145] propose to pass the attributed subgraph counts to a downstream neural network model to better compress and represent the high dimensional feature space. However, with extreme attribute shift, it may be that the downstream layers did not see certain attributed subgraph types in training enough to learn how to correctly represent them. We feel that it is better to *compress* the attributed signal *in the process of* representing the graph to handle these vertex features, the approach we take here.

There are many graph kernel methods that do not leverage subgraph counts but other features to measure graph similarity, such as the count of matching walks, e.g. Kashima et al. [61], Borgwardt et al. [21], Borgwardt and Kriegel [20]. The WL Kernel uses the WL algorithm to compare graphs [117] and will inherit the limitations of WL GNNs like inability to represent cycles. Rieck et al. [104] propose a persistent WL kernel that uses ideas from Topological Data Analysis [88] to better capture such structures when comparing graphs. Methods that do not count subgraphs will not inherit properties regarding a graph-size environment change – from our analysis of asymptotic graph theory – but all extrapolation tasks require an assumption and our framework can be applied to studying the ability of various kernel methods to extrapolate under different scenarios. Those relying on attributes to build similarities are also likely to suffer from attribute shift.

Subgraphs are studied to understand underlying mechanisms of graphs like gene regulatory networks, food webs, and the vulnerability of networks to attack, and sometimes used prognostically. A popular example investigates *motifs*, subgraphs that appear more frequently than under chance [121, 115, 85, 80, 120, 12, 5, 26, 18, 122, 34, 136]. Although the study of motifs is along a different direction and often focus on one-graph datasets, our framework learns rich latent representations of subgraphs. Another line of work uses subgraph counts as graph similarity measures, an example being matching real-world graphs to their most similar random graph generation models [101].

Other machine learning methods based on subgraphs have also been proposed. Methods like mGCMN [74], HONE [105], and MCN [73] learn representations for vertices by extending classical methods over edges to a new neighborhood structure based on subgraphs; for instance, mGCMN runs a GNN on the new graph. These methods do not exploit all subgraphs of size k and will not learn subgraph representations in a manner consistent with our extrapolation framework. Teru et al. [127] use subgraphs around vertices to predict missing facts in a knowledge base. Further examples include the Subgraph Prediction Neural network [84] that predicts subgraph classes in one dynamic heterogeneous graph; counting the appearance of edges in each type of subgraph for link prediction tasks [1]; and SEAL [149] runs a GNN over subgraphs extracted around candidate edges to predict whether an edge exists. While these methods exploit small subgraphs for their effective balance between rich graph information and computational tractability, they are along an orthogonal thread of work.

Graph Neural Networks. Among the many approaches for graph representation learning and classification, which include methods for vertex embeddings that are subsequently read-out into graph representations [15, 99, 91, 94, 66, 46, 148, 102, 82, 81, 140, 51, 25], we focus our discussion and modeling on Graph Neural Network (GNN) methods [65, 10, 50, 43, 132, 142, 86, 147, 75, 24]. GNNs are trained end-to-end, can straightforwardly provide latent graph representations for graphs of any size, easily handle vertex/edge attributes, are computationally efficient, and constitute a state-of-the-art method. However, GNNs lack extrapolation capabilities due also to their inability to learn latent representations that capture the topological structure of the graph [142, 86, 40, 110]. Relevantly, many cannot count the number of subgraphs such as triangles (3-cliques) in a graph [9, 29]. In general, our theory of extrapolating in graph tasks requires properly capturing graph structure. In our work we consider GIN [142], GCN [65] and PNA [30] as baseline GNN models. GIN and GCN are some of the most diffused models in literature. PNA generalizes different GNN models by considering multiple neighborhood aggregation schemes. Note that since we compare against PNA we do not need to consider other neighborhood aggregation schemes in GNNs, as studied in Veličković et al. [133]. To test whether more expressive models are able to extrapolate, we employ RPGIN [89]. In our experiments, we show that these state-of-the-art methods are expressive in-distribution but fail to extrapolate.

F Experiments

In this appendix we present the details of the experimental section, discussing the hyperparameters that have been tuned. Training was performed on NVIDIA GeForce RTX 2080 Ti, GeForce GTX 1080 Ti, TITAN V, and TITAN Xp GPUs.

F.1 Model implementation

All neural network approaches, including the models proposed in this paper, are implemented in PyTorch [96] and Pytorch Geometric [39].

Our GIN [142], GCN [65] and PNA [30] implementations are based on their Pytorch Geometric implementations. We consider sum, mean, and max READOUTs as proposed by Xu et al. [143] for extrapolations (denoted by XU -READOUT). For RPGIN [89], we implement the permutation and concatenation with one-hot identifiers (of dimension 10) and use GIN as before. Other than a few hyperparameters and architectural choices, we use standard choices (e.g. Hu et al. [57]) for neural network architectures. If the graphs are unattributed, we follow convention and assign a constant 1 dummy feature to every vertex.

We use the WL graph kernel implementations provided by the *graphkernels* package [123]. All kernel methods use a Support Vector Machine on scikit-learn [98].

The Graphlet Counting kernel (GC kernel), as well as our own procedure, relies on being able to efficiently count attributed or unattributed connected induced homomorphisms within the graph. We use ESCAPE [100] and R-GPM [126] as described in the main text. The source code of ESCAPE is available online and the authors of Teixeira et al. [126] provided us their code. We pre-process each graph beforehand and save the obtained estimated induced homomorphism densities. Note that R-GPM takes around 20 minutes per graph in the worst case considered, but graphs can be pre-processed in parallel. ESCAPE takes up to one minute per graph.

All the models learn graph representations $\Gamma(\mathcal{G}_{N^*}^*)$, which we pass to a L -hidden layer feedforward neural network (MLP) with softmax outputs ($L \in \{0, 1\}$ depending on the task) to obtain the prediction. For Γ_{GIN} , and Γ_{RPGIN} , we use respectively GIN and RPGIN as our base models to obtain latent representations for each k -sized connected induced subgraph. Then, we sum over the latent representations, each weighted by its corresponding induced homomorphism density, to obtain the graph representation. For $\Gamma_{1\text{-hot}}$, the representation $\Gamma_{1\text{-hot}}(\mathcal{G}_{N^*}^*)$ is a vector containing densities of each (possibly attributed) k -sized connected subgraph. To map this into a graph representation, we apply $\Gamma_{1\text{-hot}}(\mathcal{G}_{N^*}^*)^T \mathbf{W}$ where \mathbf{W} is a learnable weight matrix whose rows are subgraph representations. Note that this effectively learns a unique weight vector for each subgraph type.

We use the Adam optimizer to optimize all the neural network models. When an in-distribution validation set is available (see below), we use the weights that achieve best validation-set performance for prediction. Otherwise, we train for a fixed number of epochs.

The specifics of hyperparameter grids and downstream architectures are discussed in each section below.

F.2 Schizophrenia Task: Size extrapolation

The results of these experiments are reported in Table 1 (left). The data was graciously provided by the authors of De Domenico et al. [32], which they pre-processed from publicly available data from The Center for Biomedical Research Excellence. There are 145 graphs which represent the functional connectivity brain networks of 71 schizophrenic patients and 74 healthy controls. Each graph has 264 vertices representing spherical regions of interest (ROIs). Edges represent functional connectivity. Originally, edges reflected a time-series coherence between regions. If the coherence between signals from two regions was above a certain threshold, the authors created a weighted edge. Otherwise, there is no edge. For simplicity, we converted these to unweighted edges. Extensive pre-processing must be done over fMRI data to create brain graphs. This includes discarding signals from certain ROIs. As described by the authors, these choices make highly significant impacts on the resulting graph. We refer the reader to the paper [32]. Note that there are numerous methods for constructing a brain graph, and in ways that change the number of vertices. The measurement strategy taken by the lab can result in measuring about 500 ROIs, 1000 ROIs, or 264 as in the case we consider [49, 139, 32].

For our purposes, we wish to create an extrapolation task, where a change in environment leads to an extrapolation set that contains smaller graphs. For this, we randomly select 20 of the 145 graphs in the dataset, balanced among the healthy and schizophrenic patients, to be used as test. For each healthy-group graph in these 20 graphs, we sample (with replacement) $[0.4 \times 264]$ vertices to be removed. In average, the new size for the healthy-group graphs in these 20 graphs is 178.2.

We hold out the test graphs that are later used to assess the extrapolation capabilities. Over the remaining data, we use a stratified 5-fold cross-validation to choose the hyperparameters and to report the validation accuracy.

Once the best hyperparameters are chosen, we re-train the model on the entire training data using 10 different initialization seeds, and predict on the test.

For Γ_{GIN} and Γ_{RPGIN} , in their GNNs, the aggregation MLP of Equation (16) has hidden neurons chosen among $\{32, 64, 128, 256\}$ and number of layers (i.e. recursions of message-passing) among $\{1, 2\}$. The learning rate is chosen in $\{0.001, 0.0001\}$. The value of k is treated as a hyperparameter chosen in $\{4, 5\}$.

For $\Gamma_{\text{1-hot}}$, recall that we wish to learn the matrix \mathbf{W} whose rows are subgraph representations. We choose the dimension of the representations among $\{32, 64, 128, 256\}$ and the learning rate in $\{0.001, 0.0001\}$. The value of k is treated as a hyperparameter chosen in $\{4, 5\}$.

For the GNNs, we tune the learning rate in $\{0.01, 0.001\}$, the number of hidden neurons of the MLP in Equation (16) in $\{32, 64, 128\}$, the number of layers among $\{1, 2, 3\}$.

For all these models, we use a batch size of 32 graphs and a single final linear layer with a softmax activation as the downstream classifier. We optimize for 400 epochs.

For the graph kernels, following Kriege et al. [70], we tune the regularization hyperparameter C in SVM over the set $\{10^{-3}, 10^{-2}, 10^{-1}, 1, 10, 10^2, 10^3\}$. We tune the number of Weisfeiler-Lehman iterations of the WL kernel to be in $\{1, 2, 3, 4\}$ (see Kriege et al. [70, Section 3.1]).

F.3 Erdős-Rényi Connection Probability: Size Extrapolation

We simulated Erdős-Rényi graphs (Gnp model) using NetworkX [48]. Table 1 shows results for a single environment task (middle), where graphs in training have all size 80, and a multiple environment task (right), where training graphs have sizes in $\{70, 80\}$ chosen uniformly at random. In both cases, the test is composed of graphs of size 140. The training, validation, and test sets are fixed. The number of graphs in training, validation, and test are 80, 40, and 100, respectively. The induced homomorphism densities are obtained for subgraphs of a fixed size $k = 5$.

For $\Gamma_{\text{1-hot}}$, we hyperparameter tune the dimension of the subgraph representations in $\{32, 64, 128, 256\}$ and the learning rate in $\{0.1, 0.01, 0.001\}$.

For the GNNs and for Γ_{GIN} , and Γ_{RPGIN} , we hyperparameter tune the number of hidden neurons in the MLP of the GNN (Equation (16)) in $\{32, 64, 128, 256\}$ (GNN is used to learn the representation for k -sized subgraph for Γ_{GIN} , and Γ_{RPGIN}). The number of layers is also a hyperparameter in $\{1, 2, 3\}$ (3 layers only for the GNNs), and the learning rate in $\{0.1, 0.01, 0.001\}$. We also hyperparameter tune the presence or absence of the Jumping Knowledge mechanism from Xu et al. [141].

For IRM, we consider the two distinct graph sizes to be the two training environments. We tune the regularizer λ [7, Section 3] in $\{4, 8, 16, 32\}$, stopping at 32 because increasing its value decreased performances.

We train all neural models for 500 epochs with batch size equal to the full training data. The downstream classifier is composed by a single linear layer with softmax activations. We perform early stopping as per Hu et al. [57]. The hyperparameter search is performed by training all models with 10 different initialization seeds and selecting the configuration that achieved the highest mean accuracy on the validation data. Then, we report the mean (and standard deviation) accuracy over the training, the validation, and the test data in Table 1 (right).

For the graph kernels, following Kriege et al. [70], we tune the regularization hyperparameter C in SVM over the set $\{10^{-3}, 10^{-2}, 10^{-1}, 1, 10, 10^2, 10^3\}$. We tune the number of Weisfeiler-Lehman iterations of the WL kernel to be among $\{1, 2, 3, 4\}$ (see Kriege et al. [70, Section 3.1]).

F.4 Extrapolation performance over SBM attributed graphs

We sample Stochastic Block Model graphs (SBM) using NetworkX [48]. Each graph has two blocks, having a within-block edge probability of $\mathbf{P}_{1,1} = \mathbf{P}_{2,2} = 0.2$. The cross-block edge probability is $\mathbf{P}_{1,2} = \mathbf{P}_{2,1} \in \{0.1, 0.3\}$. The label of a graph is its cross-block edge probability, i.e., $Y = \mathbf{P}_{1,2}$.

Vertex color distributions change with train and test environments. In training, vertices in the first block are either red or blue, with probabilities $\{0.9, 0.1\}$, respectively, while vertices in the second block are either green or yellow, with probabilities $\{0.9, 0.1\}$, respectively. In test, the probability distributions are reversed: Vertices in the first block are either red or blue, with probabilities $\{0.1, 0.9\}$, respectively, and vertices in the second block are green or yellow with probabilities $\{0.1, 0.9\}$, respectively.

Table 2 shows results for the three scenarios we considered: 1. A single environment, where training graphs are of size 20 (left), 2. A multiple environment, where training graphs have size 14 or 20, chosen uniformly at random (middle), 3. A multiple environment, where training graphs are of size 20 or 30, chosen uniformly at random (right). The test is the same in all cases, and contains graphs of size 40. The number of graphs in training, validation, and test are 80, 20,

Table 4: Dataset statistics, Table from Yehudai et al. [146].

	NCI1			NCI109		
	ALL	SMALLEST 50%	LARGEST 10%	ALL	SMALLEST 50%	LARGEST 10%
CLASS A	49.95%	62.30%	19.17%	49.62%	62.04%	21.37%
CLASS B	50.04%	37.69%	80.82%	50.37%	37.95%	78.62%
NUM OF GRAPHS	4110	2157	412	4127	2079	421
AVG GRAPH SIZE	29	20	61	29	20	61

	PROTEINS			DD		
	ALL	SMALLEST 50%	LARGEST 10%	ALL	SMALLEST 50%	LARGEST 10%
CLASS A	59.56%	41.97%	90.17%	58.65%	35.47%	79.66%
CLASS B	40.43%	58.02%	9.82%	41.34%	64.52%	20.33%
NUM OF GRAPHS	1113	567	112	1178	592	118
AVG GRAPH SIZE	39	15	138	284	144	746

and 100, respectively. We obtain the induced homomorphism densities for Γ_{GIN} , Γ_{RPGIN} , $\Gamma_{\text{1-hot}}$ for a fixed subgraph size $k = 5$.

For the GNNs and for Γ_{GIN} and Γ_{RPGIN} , we choose the number of hidden neurons in the MLP of the GNN (Equation (16)) in $\{32, 64, 128, 256\}$, the number of layers in $\{1, 2, 3\}$ (3 layers only for the GNNs) and hyperparameter tune the presence or absence of the Jumping Knowledge mechanism from Xu et al. [141]. We add the regularization penalty in Equation (9) for Γ_{GIN} and Γ_{RPGIN} in this experiments. For Γ_{GIN} and Γ_{RPGIN} , we choose the learning rate in $\{0.01, 0.001\}$ and the regularization weight in $\{0.1, 0.15\}$. For the GNNs we choose the learning rate in $\{0.1, 0.01, 0.001\}$.

For IRM, we consider the two distinct graph sizes to be the two training environments. We can not treat vertex attributes as environment here since we only have a single vertex-attribute distribution in training. We tune the regularizer λ [7, Section 3] in $\{4, 8, 16, 32\}$, stopping at 32 because increasing its value decreased performances.

For $\Gamma_{\text{1-hot}}$, we hyperparameter tune the dimension of the subgraph representations in $\{32, 64, 128, 256\}$ and the learning rate in $\{0.01, 0.001\}$.

We optimize all neural models for 500 epochs with batch size equal to the full training data. We use a single layer with softmax outputs as the downstream classifier. We perform early stopping as per Hu et al. [57]. The hyperparameter search is performed by training all models with 10 different initialization seeds and selecting the configuration that achieved the highest mean accuracy on the validation data. Then, we report the mean (and standard deviation) accuracy over the training, the validation, and the test data in Table 2.

For the graph kernels, following Kriege et al. [70], we tune the regularization hyperparameter C in SVM over the set $\{10^{-3}, 10^{-2}, 10^{-1}, 1, 10, 10^2, 10^3\}$. We tune the number of Weisfeiler-Lehman iterations of the WL kernel to be among $\{1, 2, 3, 4\}$ (see Kriege et al. [70, Section 3.1]).

F.5 Extrapolation performance in real world tasks that violate our causal model

Results are reported in Table 3. We use the datasets from Morris et al. [87], split into train, validation and test as proposed by Yehudai et al. [146]. In particular, train is obtained by considering the graphs with sizes smaller than the 50-th percentile, and test those with sizes larger than the 90-th percentile. Additionally, 10% of the training graphs is held out from training and used as validation. For statistics on the datasets and corresponding splits, see Yehudai et al. [146].

We obtain the homomorphism densities for a fixed subgraph size $k = 4$. We observed that larger subgraph sizes, $k \geq 5$, implies a larger number of distinct subgraphs and consequently a smaller proportion of shared subgraphs in different graphs. To further reduce the number of distinct subgraphs seen by the models, we only consider the most common subgraphs in training and validation when necessary. Specifically, for NCI1 and NCI109, we only use the top 100 subgraphs (out of a total of around 300), and for DD only the 30k most common (out of a total of around 200k). For PROTEINS we keep all the distinct subgraphs (which are around 180).

For the GNNs, we follow the setup proposed in Yehudai et al. [146], where all the GNNs have 3 layers and a final classifier composed of a feedforward neural network (MLP) with 1 hidden layer and softmax outputs. We tune the batch size in $\{64, 128\}$, the learning rate in $\{0.01, 0.005, 0.001\}$ and the network width in $\{32, 64\}$. For Γ_{GIN} and Γ_{RPGIN} , the setup is the same, except for the number of GNN layers that is set to 2. For DD we use a fixed batch size of 256 to reduce the number of times the subgraphs are passed to the network, in order to speed up training.

For $\Gamma_{\text{1-hot}}$, we choose the batch size in $\{64, 128\}$, the learning rate in $\{0.01, 0.005, 0.001\}$ and the dimension of the subgraph representations in $\{32, 64\}$.

For IRM we tune the regularizer λ [7, Section 3] in $\{8, 32, 128, 512\}$. The two environments are considered to be graphs with size smaller than the median size in the training graphs and larger than the median size in the training graphs, respectively.

To mitigate the imbalance between classes in training, we reweight the classes in the loss with the training proportions for each class. We train all neural models for 1000 epochs using early stopping as per Hu et al. [57]. We test the models on the epoch achieving the highest mean Matthew Correlation Coefficient on validation because of the significant class imbalance in the test, see Table 4.

For the graph kernels, following Kriege et al. [70], we tune the regularization hyperparameter C in SVM over the set $\{10^{-3}, 10^{-2}, 10^{-1}, 1, 10, 10^2, 10^3\}$. We fix the number of Weisfeiler-Lehman iterations of the WL kernel to 3 (see Kriege et al. [70, Section 3.1]), which is comparable to the 3 GNN layers.